Investigation of intracellular delivery of NuBCP-9 by conjugation with oligoarginines peptides

（細胞膜透過性 oligoarginines ペプチドによるアポトーシス誘導性 NuBCP-9 ペプチドの細胞内送達に関する研究）

2018

WANG WEI

Content

Preface

Drug therapy is an indispensable part of clinical practices aimed at overcoming cancer and can be applied independently or combined with other strategies. Any conventional therapeutic approach must mediate tumor cell death while minimizing side-effects. In general, traditional chemotherapeutic drugs lead to systemic toxicity resulting from non-specific distribution in the body. Pro-apoptotic peptides are other promising alternatives to chemotherapy. They could effectively and specifically induce cancer cell death. However, in contrast to small molecular drugs, most of peptide drugs are membrane impermeable, restricting their uptake and activity. Therefore, additional vectors or components are required to ensure their passage through the cell membrane.

Cell penetrating peptides (CPPs) are commonly used for intracellular delivery of therapeutic peptides, due to high cellular uptake efficiency with a simpler synthesis procedure and conjugation method, especially in the case of cargo therapeutic peptides conjugated by amino acid linkers. As synthetic cationic CPPs, oligoarginines (Rn) are widely used due to its high uptake capacity.

Targeting Bcl-2 is an efficient strategy for specifically inducing apoptosis in cancer cells. Many Bcl-2-targeted peptides have been reported in the literature. Among them, NuBCP-9, a Nur77-derived peptide composed of 9 amino acids (FSRSLHSLL), has been reported to specifically interact with the anti-apoptotic protein Bcl-2 to induce apoptosis. However, when utilizing R8 for delivering NuBCP-9, not only promoted uptake efficiency but also enhanced non-specific cytotoxicity (unrelated with Bcl-2) have been published in following study. Due to Rn with different length possess different uptake efficiency, it is worthy to investigate the influence of NuBCP-9 conjugation on uptake efficiency of different Rn. Furthermore, related to such enhancement of uptake efficiency, the uptake mechanism is still undiscussed.

On the other hand, effective biological based therapy not only depends on the cellular uptake of therapeutic agent via delivery vectors but also on the ability to escape

from endosomes to reach intracellular target for eliciting its effect. Especially for biological macromolecules, it will be faced the acidic and enzymic endosomal environment and endosome membrane barrier. Those suggest that it is essential to evaluate the biological effect of therapeutic reagent for confirming efficient cytosolic delivery.

In present study, I firstly investigated the influence of NuBCP-9 conjugation on the cellular uptake, distribution and uptake pathways of Rn. For finding suitable length of Rn to deliver NuBCP-9 into cells then interact with Bcl-2, the cytotoxicity including membrane disrupted effect and apoptosis that caused by NuBCP-9-Rn conjugates were evaluated for confirming the efficient cytosolic delivery of peptides. Rn and NuBCP-9-Rn (n= 0, 6, 8, 10, 12 and 14) conjugates were synthesized through solid phase peptides synthesize method and purified by RP-HPLC. For evaluating uptake, all the peptides were labelled with fluorescein-5-maleimide, and were confirmed by RP-HPLC and MALDI-TOF-MS. The cellular uptake and distribution were investigated using flow cytometry and confocal laser scanning microscopy. The influence of three typical uptake inhibitors and 4℃ treatment on the uptake behavior were evaluated to discuss the uptake pathway of Rn and NuBCP-9-Rn conjugates. The cell viability of all unlabeled peptides was measured with WST-8 assay. For distinguishing the non-specific membrane disrupted effect and Bcl-2 related apoptosis, LDH assay and Annexin V-FITC/PI staining were conducted. I hope the information in this study will be valuable in the design of therapeutic peptide conjugated with oligoarginines for anti-cancer therapy.

Chapter I

Investigation of cellular uptake, distribution and uptake pathways of Rn and NuBCP-9-Rn conjugates

1. Introduction

Pro-apoptotic peptides are promising alternatives to chemotherapeutic drugs because they could induce cancer cell death specifically with reduced systemic side effect[1,2]. However, in contrast to small molecular drugs, most of therapeutic peptides are membrane impermeable, restricting their uptake and hindering their clinical use. Until now, many approaches have been studied for intracellular delivery of therapeutic peptides including cell penetrating peptides (CPPs)[3–5], liposomes[6], polymeric carriers[7] and other nano-system[8–10]. The development of nanocarriers may encounter complex synthesis process and solvent residue issue[11,12], while CPPs exhibit high cellular uptake efficiency with a simpler synthesis procedure and conjugation method, especially in the case of cargo peptides conjugated by amino acid linkers[13]. Thus, CPPs are commonly used for intracellular delivery of therapeutic peptides.

CPPs are also known as protein transduction domains (PTDs), which has been utilized for introducing various kinds of exogenous substances into cells with high efficiency and relative low cytotoxicity[14]. HIV trans-activating transcriptional activator protein (TAT) was the firstly discovered CPPs 30 years before[15]. After that, numerous kinds of CPPs has been reported[16–18]. Among them, cationic CPPs are most commonly used classes, which are highly positive charged from composition of arginine and/or lysine. As synthetic cationic CPPs, oligoarginines (Rn) showed significant higher uptake capacity than oligolysine[19]. One possible reason is the different affinity with cell membrane between arginine and lysine. The affinity could decide the cell surface concentration of peptides which is crucial for effective uptake. Unlike epsilon-amino group contained in lysine, the guanidino group of arginine may form dual hydrogen bonds with the negative groups on cell surface via electrostatic interactions, such as sulfate, and phosphate[20]. In general, the uptake efficiency of Rn can be affected by the numbers of arginine comprising it[19].

Until now, two major uptake mechanisms of Rn have been reported, namely, endocytosis and direct membrane transduction. In addition, three typical endocytosis pathways: clathrin-mediated endocytosis, caveolae-mediated endocytosis and macropinocytosis have been suggested as the uptake pathways of Rn, which depended

on the treatment concentrations, cell lines and also the properties of cargos[21–24]. Many researches showed that hydrophobic modification on CPPs promoted the uptake[25–28], while such enhancement had different effect on the uptake pathways of CPPs. Compare with octaarginine (R8), R8 modified with higher portion of hexanoyl group directly penetrated the cell membrane[29], while the uptake of R8 modified with FFLIPKG peptide mainly mediated by endocytosis[26]. Meanwhile, different kinds of CPPs showed various degrees on uptake capacity with same hydrophobic modification, which suggests the importance of the intrinsic uptake efficiency of the CPPs themselves[25].

NuBCP-9, a Nur77-derived pro-apoptotic peptide composed of 9 amino acids (FSRSLHSLL), is used in this research. Firstly, Kolluri *et al.* used R8 to facilitate intracellular delivery of NuBCP-9 and proved NuBCP-9-R8 induced apoptosis in Bcl-2 overexpressing cancer cells but be harmless in normal cells[30]. Later study demonstrated that the uptake efficiency of R8 can be significantly enhanced by conjugation with NuBCP-9 accompany with magnified non-specific cytotoxicity of R8 that was unrelated with Bcl-2[31]. Due to Rn with different length possess different uptake efficiency, it is worthy to investigate the influence of NuBCP-9 conjugation on uptake efficiency of different Rn. Furthermore, related to such enhancement of uptake efficiency, the uptake mechanism is still undiscussed.

Therefore, in this chapter, I investigated the uptake characteristics of NuBCP-9 conjugation of various Rn that differed in the numbers of arginine comprising them. In addition, I compared the uptake pathways taken by various Rn and NuBCP-9-Rn (0, 6, 8, 10, 12 and 14) conjugates in a Bcl-2 overexpressing cell line, MDA-MB-231 (human breast cancer cells)[32–34]. All the peptides were produced through solid phase peptides synthesis method and RP-HPLC purification. Glycine-Cysteine segment was added at the C-terminus of peptides which allow fluorescein-5-maleimide label with peptides via thiol-maleimide reaction. The fluorescence intensity was analyzed under flow cytometry with fluorescein (FI) labelled peptides, and subcellular distribution of peptides was observed under confocal laser scanning microscopy (CLSM).

2. Materials and methods

2.1. Materials and Instruments

Name	Source
Rink amide AM resin (100-200 mesh)	Novabiochem, Merck Millipore, Germany
Fmoc-Amino Acid-Protection group*	Merck Millipore, Germany
Piperidine	Wako, Japan
Acetic anhydride (Ac_2O)	Wako, Japan
Hydroxybenzotriazole (HOBt)	Peptide Institute, Japan
O-(1H-Benzotriazol-1-yl)-*N*,*N*,*N*′,*N*′-tetramethyluronium hexafluorophosphate (HBTU)	Novabiochem, Merck Millipore, Germany
N,*N*-Diisopropylethylamine (DIEA)	Novabiochem, Merck Millipore, Germany
Triisopropylsilane (TIS)	Novabiochem, Merck Millipore, Germany
Ethanedithiol (EDT)	Novabiochem, Merck Millipore, Germany
Kaiser Test kits	Self-made kits in PI lab
Trifluoroacetic acid (TFA)	Watanabe Chemical Industries, Japan
4-(2-Hydroxyethyl)-1-piperazineethanesulfonic acid (HEPES)	Dojindo Molecular Technologies, Japan
EDTA·2Na	Dojindo Molecular Technologies, Japan
Fluorecine-5-maleimide (F5M)	TCI chemicals, Japan
Tris (2-carboxyethyl) phosphine hydrochloride (TCEP·HCl)	Sigma-Aldrich, Germany
4-azidobenzoic acid (4-ABA)	TCI chemicals, Japan
Dimethylformamide (DMF)	Watanabe Chemical Industries, Japan
Dichloromethane (DCM)	Nacalai Tesque. Inc., Japan
Methanol	Kanto Chemicals Co., Japan
Diethyl ether (Et_2O)	Wako, Japan
Acetonitrile (ACN)	Sigma-Aldrich, Germany
COSMOSIL Packed Column 5C_{18}-AR-II (20 ID × 250 mm)	Nacalai Tesque. Inc., Japan
COSMOSIL Packed Column 5C_{18}-AR-II (4.6 ID × 250 mm)	Nacalai Tesque. Inc., Japan
RPMI-1640	Wako, Japan
Heat-inactivated fetal bovine serum (FBS)	AusGene X, Australia
Penicillin	Wako, Japan
Streptomycin	Wako, Japan
Trypsin-EDTA	Wako, Japan
Heparin sodium (5000 Unit/5mL)	Mochida Pharmaceutical Co.
Chlorpromazine (CPZ)	Wako, Japan
Genistein	Sigma-Aldrich, Germany
5-(*N*-ethyl-*N*-isopropyl) amiloride (EIPA)	Sigma-Aldrich, Germany
Cell Counting Kit-8	Dojindo Molecular Technologies, Japan
LysoTracker Red	Thermo Scientific, United States
Hoechst 33342	Thermo Scientific, United States
24-well and 96-well cell culture plate	Violamo, Japan
8-well Nunc Lab-Tek II chambered coverglass	Thermo Scientific, United States

Falcon 5 ml round-bottom tube, with cell strainer cap	Corning, United States
pH meter F-22	Horiba, Japan
Nitrogen (N_2) supplier MODEL 02B	System Instruments Co., Japan
Rotary evaporator L-FB145	Tokyo Rikakikai Co., Japan
High Speed Refrigerated Centrifuge M6000	Kubota, Japan
Rotary shaker N-500	Kokusan Chemical Co., Japan
Eyela lyophilizer FDU-1200	Tokyo Rikakikai Co., Japan
HPLC LC-20AD	Shimadzu Co., Japan
MALDI-TOF-MS	Bruker Daltonics Ultraflex, United State
High Speed Refrigerated Centrifuge 3520	KUBOTA CO., Japan
iMark™ microplate absorbance reader	Bio-Rad Laboratories, United State
BD LSRFortessa X-20 flow cytometer	BD bioscience, United States
LSM 710	Carl Zeiss, Germany

* Protection group based on the kind of amino acids.

2.2. Cell culture

MDA-MB-231 cells (human breast cancer cell line) were purchased from the European Collection of Authenticated Cell Cultures (ECACC) and were cultured in RPMI-1640 supplemented with 10% heat-inactivated FBS, 100 U/mL penicillin, and 100 mg/mL streptomycin. Subculture the cells 2 or 3 times a week. The population doubling time (PDT) was around 20 h.

2.3. Synthesis, purification and structure identification of peptide

All the peptides in this study were synthesized by Fmoc (9-fluorenylmethyloxy-carbonyl) solid phase peptide synthesis method using Rink amide resin and Fmoc-L-amino acids (Fmoc-AA). For 0.05 mmol synthesis scale (1 equiv.), 121.95 mg Rink amide resin (loading: 0.41 mmol/g) was swelled overnight by 2 mL DMF in synthesis column. After removing DMF, then 2 mL 20% piperidine (*v*/*v*) contained DMF was added into column for deprotecting Fmoc group and keep mild shaking for 20 min. After reaction, filtration and washing the resin with DMF (2 mL, 4 × 1 min) were conducted. Dissolve 4 equiv. Fmoc-AA which need to be coupled in 5 mL tube with 0.5 mL DMF, then mix with 1 mL 4 equiv. HOBt/HBTU contained DMF and 1 mL 8 equiv. DIEA contained DMF for about 5 min before coupling step to activate the carboxyl group of Fmoc-AA. After removing DCM, the activated Fmoc-AA mixture

was added to column and 30 min mild shaking was proceeded for coupling with amino acids. After filtration, the resin was washed with DMF (2 mL, 2 × 1 min) and following with DCM (2 mL, 2 × 1 min). The reaction was checked with Kaiser Test kits under boiled water. If the Kaiser Test showed positive result (resin showed blue or deep red color), the coupling procedure was repeated until it being negative. When the Kaiser Test showed negative result (resin showed colorless), 2 mL 25% Ac_2O (*v*/*v*) contained DCM was used for acetylating unreacted amino groups on resin throughout the synthesis (mild shaking for 5 min). After filtration, the resin was washed with DCM (2 mL, 2 × 1 min) and following with DMF (2 mL, 2 × 1 min). Procedures including deprotecting, activating, coupling- Kaiser Test, and acetylating steps were repeated for coupling of each amino acid. After all coupling for desired sequence, deprotection of Fmoc group of amino acid at N-terminus of peptides was conducted using 2 mL 20% piperidine (*v*/*v*) contained DMF for 20 min mild shaking. After reaction, filtration and washing the resin with DMF (2 mL, 4 × 1 min) were conducted. For acetylating N-terminal of peptides, 1.8 mL 10% Ac_2O (*v*/*v*) contained DMF was added and kept shaking for 5 min, then 200 μL 6 equiv. DIEA contained DMF was added and continuous shaking for 25 min. After filtration, the resin was washed with DMF (2 mL, 2 × 1 min), following wash with DCM (2 mL, 2 × 1 min) and methanol (2 mL, 5 × 1 min). Dry in desiccator over 2 h. The flow chart shown in Fig.1.

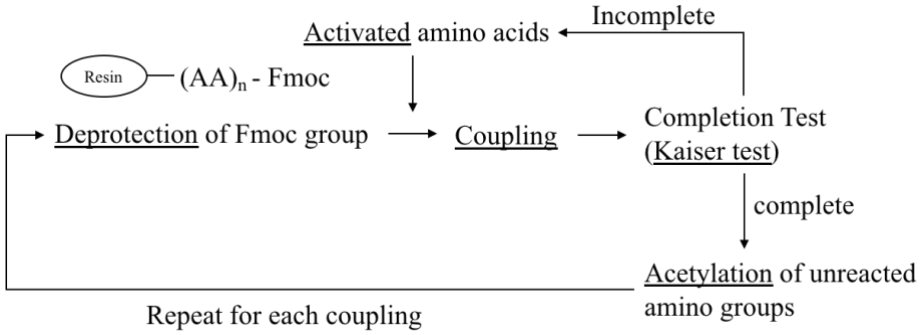

Fig.1 Flow chart of Fmoc-solid phase peptide synthesis.

The cleavage step used 2350 μL TFA/25 μL TIS/62.5 μL H_2O/62.5 μL EDT (94 / 1 / 2.5 / 2.5) cocktail. After shaking for 3 h, filter the resin and collect the cleavage solution into 50 mL tube. Filtration and washing the resin three times with 1.5 mL TFA was conducted and collected TFA solution was added to the same 50 mL tube. Then

evaporated the peptides contained TFA solution to a little volume under N_2 circulation. 30 mL ice-cold Et_2O was used for precipitating the peptides. Then centrifuge the tube with 26,300 g at 4 ℃ for 5 min using High Speed Refrigerated Centrifuge M6000. Remove the Et_2O and repeat washing the precipitated peptides with 30 mL ice-cold Et_2O twice. Dry the crude peptides in desiccator over 3 h. The powder with pale yellow color was collected as crude peptides, store in - 30 ℃ refrigerator before purification.

After dissolving appropriate crude peptides in 0.4 mL acetonitrile/H_2O mixture, peptides were purified using RP-HPLC with a COSMOSIL Packed Column 5C18 -AR-II (20 ID × 250 mm). Mobile phase: A) 0.05% TFA in ACN B) 0.05% TFA in diH_2O. Flow rate: 5 mL/min. Gradient elution was used for separating products. Basic gradient of B was 90 to 30% over 30 min, and it was adjusted for acceptable separation based on the hydrophobicity of each peptide. The mobile phase of the main peak was collected and then evaporated to remove the ACN under 45 ℃ water bath. Then the purified peptide solution was lyophilized after pre-freezing in - 30 and - 75 ℃ refrigerator. Part of peptides were dissolved in sterilized distilled water to a stock concentration of 1 mg/mL, aliquoted and frozen at - 30 ℃ until needed.

The purity of peptide was evaluated by RP-HPLC using COSMOSIL Packed Column 5C18-AR-II (4.6 ID × 250 mm). Mobile phase: A) 0.05% TFA in ACN B) 0.05% TFA in diH_2O. Gradient elution was used for each peptide. Basic gradient of B was 90 to 30% over 30 min, and it was adjusted for better separation based on the hydrophobicity of each peptide. Flow rate: 0.8 mL/min. Detecting wavelength: 215 nm or 220 nm.

For confirming the structure of target peptide, Matrix-Assisted Laser Desorption/ Ionization Time of Flight Mass Spectrometry (MALDI-TOF-MS) was used for detecting the molecular weight of each peptide. Briefly, the matrix solution was the saturated solution of α-Cyano-4-hydroxycinnamic acid (CHCA) in ACN. 2 μL matrix solution was deposited on the sample spot of target plate and dried, totally for 3 times. 1 mg /mL peptide solution (in diH_2O) was mixed with matrix solution at 1 : 1 (*v*/*v*) ratio. Then add 2 μL such mixture on the same sample spot, dried with blower (cold air) for co-crystalizing the peptides with matrix on the target position. Repeat depositing

samples for 2 times. After preparing samples on target plate, detected the molecular weight of analyte with MALDI-TOF-MS.

2.4. Fluorescence labelling of peptides

2.4.1. The influence of reaction pH on the labelling reaction

1 M HCl and 1 M NaCl solution were used to adjust the pH of 150 mM NaCl supplemented 50 mM HEPES buffer, the final pH was 6.8, 7.0, 7.3 and 7.6. TCEP·HCl was dissolved in diH_2O prior to use. Dissolve purified AA-R8 in each 50 mM HEPES buffer (1 equiv.) with different pH, then 3 equiv. TCEP·HCl in diH_2O was added and keep shaking for 30 min at room temperature. Fluorescein-5-maleimide was dissolving in DMF (4 mg/mL) prior to use. Then mix 2 equiv. F5M in DMF and 10 mM EDTA·2Na with peptides reaction solution, protect reaction from light and keep shaking for 1.5 h at room temperature. The finial reaction mixture was analyzed with RP-HPLC using a COSMOSIL Packed Column 5C18 -AR-II (20 ID × 250 mm). Mobile phase: A) 0.05% TFA in ACN B) 0.05% TFA in diH_2O. Gradient of B was 90 to 35% over 30 min. Flow rate: 5 mL/min. Detecting wavelength: 280 nm.

2.4.2. The influence of TCEP on the labelling reaction

Purified NuBCP-9-R8 conjugate (1 equiv.) or TCEP·HCl were dissolved in pH 7.0 150 mM NaCl contained 50 mM HEPES buffer prior to use, respectively. Then 0, 2, 5 equiv. TCEP·HCl (4 mg/mL in hepes buffer) was added into peptides solution and keep shaking for 30 min at room temperature, respectively. Fluorescein-5-maleimide was dissolved in DMF (4 mg/mL) prior to use. Then mix 2 equiv. F5M in DMF and 10 mM EDTA·2Na with peptides reaction solution, protect reaction from light and keep shaking for 1.5 h at room temperature. The final concentration of peptides was controlled to be 2 mg/mL. 250 μL finial reaction mixture was analyzed with RP-HPLC using a COSMOSIL Packed Column 5C18 -AR-II (20 ID × 250 mm). Mobile phase: A) 0.05% TFA in ACN B) 0.05% TFA in diH2O. Gradient of B was 85 to 35% over 30 min. Flow rate: 5 mL/min. Detecting wavelength: 280nm.

2.4.3. The influence of 4-ABA on the labelling reaction

Dissolve purified R8 (1 equiv.) or TCEP·HCl in pH 7.0 150 mM NaCl contained 50 mM HEPES buffer prior to use, respectively. Then 5 equiv. TCEP·HCl (4 mg/mL in HEPES buffer) was added into peptides solution and keep shaking for 30 min at room temperature. Add 0 or 10 equiv. 4-ABA (20 mg/mL in methanol) into peptides reaction solution and keep shaking for 30 min at room temperature. Dissolve fluorescein-5-maleimide in DMF (4 mg/mL) prior to use. Then add 2 equiv. F5M in DMF and 10 mM EDTA·2Na into peptides reaction solution, protect reaction from light and keep shaking for 1.5 h at room temperature. The final concentration of peptides was controlled to be 2 mg/mL. 250 μL finial reaction mixture was analyzed with RP-HPLC using a COSMOSIL Packed Column 5C18 -AR-II (20 ID × 250 mm). Mobile phase: A) 0.05% TFA in ACN B) 0.05% TFA in diH_2O. Gradient of B was 90 to 45% over 30 min. Flow rate: 5 mL/min. Detecting wavelength: 280 nm.

2.5. Reaction, purification and structure identification of fluorescein labelled peptide

Dissolve purified peptides (1 equiv.) or TCEP·HCl in pH 7.0 150 mM NaCl contained 50 mM HEPES buffer prior to use, respectively. Then 5 equiv. TCEP (4 mg/mL in HEPES buffer) was added into peptides solution and keep shaking for 30 min at room temperature. Add 10 equiv. 4-ABA (20 mg/mL in methanol) into peptides reaction solution and keep shaking for 30 min at room temperature. Dissolve fluorescein-5-maleimide in DMF (4 mg/mL) prior to use. Then add 2 equiv. F5M in DMF and 10mM EDTA·2Na into peptides reaction solution, protect reaction from light and keep shaking for 1.5 h at room temperature or keep in 4 ℃ refrigerator overnight. The final concentration of peptides was controlled to be 2 mg/mL. Purify the finial reaction mixture with RP-HPLC using a COSMOSIL Packed Column 5C18 -AR-II (20 ID × 250 mm). Mobile phase: A) 0.05% TFA in ACN B) 0.05% TFA in diH_2O. Gradient elution was used for each peptide. Flow rate: 5 mL/min. Detecting wavelength: 280 nm. The purity and molecular weight were also confirmed under RP-HPLC and MALDI-TOF-MS.

2.6. Cellular uptake of Rn and NuBCP-9-Rn conjugates

2.6.1. Influence factors on cellular uptake of peptides (heparin washing step, incubation time and treatment concentration)

5.0×10^4 /cm^2 MDA-MB-231 cells (in 0.5 mL culture medium) were seeded into 24-well plates and cultured for 24 h. Then incubated cells in 0.5 mL culture medium containing R8 or NuBCP-9-R8 conjugate peptides at 37 ℃ for indicated time with 5% CO_2. After washing with 0.5 mL phosphate-buffered saline (PBS), the cells were harvested and centrifuged at 300 g for 3 min at 4 ℃. After washing twice with 0.5 mL ice-cold PBS supplemented with 20 units/mL of heparin or ice-cold PBS only, cells were re-suspended in PBS and analyzed using BD LSRFortessa X-20 flow cytometer. 10,000 events were taken for each sample. The blue 488-nm laser was used for excitation of FITC and its fluorescence intensity was detected by a 525/30 BP filter.

2.6.2. Cellular uptake of Rn and NuBCP-9-Rn conjugates

5.0×10^4 /cm^2 MDA-MB-231 cells (in 0.5 mL culture medium) were seeded into 24-well plates and cultured for 24 h. Then incubated cells in 0.5 mL culture medium containing indicated peptides at 37 ℃ for 30min with 5% CO_2. After washing with 0.5 mL phosphate-buffered saline (PBS), the cells were harvested and centrifuged at 300 g for 3 min at 4 ℃. After washing twice with 0.5 mL ice-cold PBS supplemented with 20 units/mL heparin, cells were re-suspended in PBS and analyzed using BD LSRFortessa X-20 flow cytometer. 10,000 events were taken for each sample. The blue 488-nm laser was used for excitation of FITC and its fluorescence intensity was detected by a 525/30 BP filter.

2.6.3. Cellular distribution of Rn and NuBCP-9-Rn conjugates

5.0×10^4 /cm^2 MDA-MB-231 cells (in 200 μL culture medium) were seeded into 8-well Nunc Lab-Tek II chambered coverglass and incubated for 24 h. 50 nM LysoTracker Red and 5 μg/mL Hoechst 33342 were added into culture medium for staining late endosomes/lysosomes and nuclei, respectively. Then, the cells were incubated in such culture medium containing 2 μM or 10 μM peptides at 37 ℃ for 30

min. Washing twice with 200 μL ice-cold PBS supplemented with 20 units/mL of heparin, then add 200 μL mL ice-cold culture medium and keep the chambered coverglass on ice before observing. 1 μL of 0.4% trypan blue was added into the chamber, then observed cells immediately using LSM 710 at an excitation wavelength 488 nm (Ar laser) for peptides, 543 nm (He-Ne laser) for LysoTracker Red and 405 nm (UV laser) for Hoechst 33342.

2.7. Investigation of uptake mechanism of NuBCP-9-R8 conjugate by amino acid replacement of NuBCP-9

NuBCP-9-R8, FA-R8 and AA-R8 conjugate peptides were used in this part. The experiment procedures under flow cytometer was same with the description in 2.6.2.

2.8. Uptake pathways of Rn and NuBCP-9-Rn conjugates

2.8.1. Influence of treatment dose of uptake inhibitors on cell survival

4.5×10^4 /cm^2 MDA-MB-231 cells (in 100 μL culture medium) were seeded into 96-well plates and cultured for 24 h. Then, the cells were incubated in 100 μL culture medium containing uptake inhibitors with various concentration for 1 h at 37 ℃ with 5% CO_2. After incubation, washed cells with PBS for 2 times. Then 100 μL Cell Counting Kit-8 (CCK-8) contained fresh medium (CCK-8 : medium = 1 : 10 *v*/*v*) was added and keep incubating cells for 3 h at 37 ℃ with 5% CO_2. Measure the absorbance at 450 nm using microplate absorbance reader.

2.8.2. Influence of uptake inhibitors on cellular uptake of Rn and NuBCP-9-Rn conjugates

5.0×10^4 /cm^2 MDA-MB-231 cells (in 0.5 mL culture medium) were seeded into 24-well plates and cultured for 24 h. Change culture medium with 0.4 mL uptake inhibitors contained culture medium (chlorpromazine, EIPA, and genistein at concentrations of 50, 100, and 200 μM, respectively), pre-incubated cells for 30 min at 37 ℃ with 5% CO_2. Then, the cells were incubated with 2 μM or 10 μM peptides in the absence or presence of inhibitors in 0.4 mL medium for 30 min at 37 ℃ with 5% CO_2.

The following steps were same with the description in 2.6.2.

2.8.3. Influence of uptake inhibitors on cellular distribution of Rn and NuBCP-9-Rn conjugates

5.0×10^4 /cm^2 MDA-MB-231 cells (in 200 μL culture medium) were seeded into 8-well Nunc Lab-Tek II chambered coverglass and incubated for 24 h. Change culture medium with uptake inhibitors contained fresh medium (chlorpromazine, EIPA, and genistein at concentrations of 50, 100, and 200 μM, respectively), pre-incubated cells for 30 min at 37 ℃ with 5% CO_2. 50 nM LysoTracker Red and 5 μg/mL Hoechst 33342 were added into culture medium for staining late endosomes/lysosomes and nuclei, respectively. Then, 200 μL such culture medium containing 2 μM or 10 μM peptides was added in the absence or presence of inhibitors, and the cells were incubated for 30 min at 37 ℃ with 5% CO_2. The following steps were same with the description in 2.6.3.

2.8.4. Influence of temperature on cellular uptake of Rn and NuBCP-9-Rn conjugates

5.0×10^4 /cm^2 MDA-MB-231 cells (in 0.5 mL culture medium) were seeded in 24-well plate for 24 h. Then balanced the cells in 4 ℃ refrigerator for 30min. Then, the cells were incubated in 0.5 mL ice-cold culture medium containing peptides in 4 ℃ refrigerator for 30 min. The following steps were same with the description in 2.6.2.

2.8.5. Influence of temperature on cellular distribution of Rn and NuBCP-9-Rn conjugates

5.0×10^4 /cm^2 MDA-MB-231 cells (in 200 μL culture medium) were seeded into Nunc Lab-Tek II chambered coverglass for 24 h. Then balanced the cells in 4 ℃ refrigerator for 30 min. Then, the cells were incubated in 200 μL ice-cold culture medium containing peptides in 4 ℃ refrigerator for 30min. The following steps were same with the description in 2.6.3. Observed cells using LSM 710 at an excitation wavelength 488 nm (Ar laser) for peptides.

2.9. Statistical Analysis

All comparisons of mean values were performed using analysis of variance test (ANOVA). Unpaired t-test was utilized for two-group comparisons. Multiple comparisons among all groups were performed using two-way ANOVA with Bonferroni test. For comparisons between control and treatment groups, Dunnett test was used. Results yielding a p value less than 0.05 were considered statistically significant.

3. Results

3.1. Synthesis, purification and structure identification of peptide

Solid phase peptide synthesis method was used for peptide synthesizing[35,36]. Resins are utilized as support to link with first C-terminal amino acid via covalent bond, then the following amino acid can be coupled one at a time in as stepwise manner. As completely insoluble particles, resin linked peptides can be easily filtered and washed for removing reagents and by-products, which is time-saving and easy-handling. Cleavage of the peptides with desired sequence from resin can be achieved by treatment with 95% TFA. RP-HPLC is versatile tool for purifying peptides on the basis of hydrophobicity. Peptides can be eluted and separated by changing gradient slope of organic solvent. Additional 0.05% - 0.1% TFA in mobile phase could help to minimize peak broadening[37].

As one kind of soft-ionization techniques, Matrix-assisted laser desorption/ionization time-of-flight mass spectrometry (MALDI-TOF-MS) is widely used for analyzing the molecular weight of biological molecules[38]. Thus, in this section all the peptides (Tab.1) were synthesized via SPPS, purified via RP-HPLC and confirmed via MALDI-TOF-MS.

From the results, all the peptides obtained over 90% purity after RP-HPLC purification (Fig. 2). Besides, the molecular weight that observed under MALDI-TOF-MS was similar with the calculated value of each peptides (Tab. 2).

Tab. 1 Name and sequence of peptides used in this study. All peptides consisted of L-form amino acids. X represents 6 - aminohexanoic acid. For uptake investigation, fluorescein (FI) was conjugated with the cysteine (C) of peptides.

Unlabeled peptides	Sequence
R6	Ac - RRRRRRGC - NH_2
R8	Ac - RRRRRRRRGC - NH_2
R10	Ac - RRRRRRRRRRGC - NH_2
R12	Ac - RRRRRRRRRRRRGC - NH_2
R14	Ac - RRRRRRRRRRRRRRGC - NH_2
NuBCP-9	Ac - FSRSLHSLLGC - NH_2
NuBCP-9-R4	Ac - FSRSLHSLL - GGG- RRRRGC - NH_2
NuBCP-9-R6	Ac - FSRSLHSLL - GGG- RRRRRRGC - NH_2
NuBCP-9-R8	Ac - FSRSLHSLL - GGG- RRRRRRRRGC - NH_2
NuBCP-9-R10	Ac - FSRSLHSLL - GGG- RRRRRRRRRRGC - NH_2
NuBCP-9-R12	Ac - FSRSLHSLL - GGG- RRRRRRRRRRRRGC - NH_2
NuBCP-9-R14	Ac - FSRSLHSLL - GGG- RRRRRRRRRRRRRRGC - NH_2
NuBCP-9-GX-R8	Ac - FSRSLHSLL - GX- RRRRRRRRGC - NH_2
FA-R8	Ac - FSRSLHSLA - GX- RRRRRRRRGC - NH_2
AA-R8	Ac - ASRSLHSLA - GX- RRRRRRRRGC - NH_2

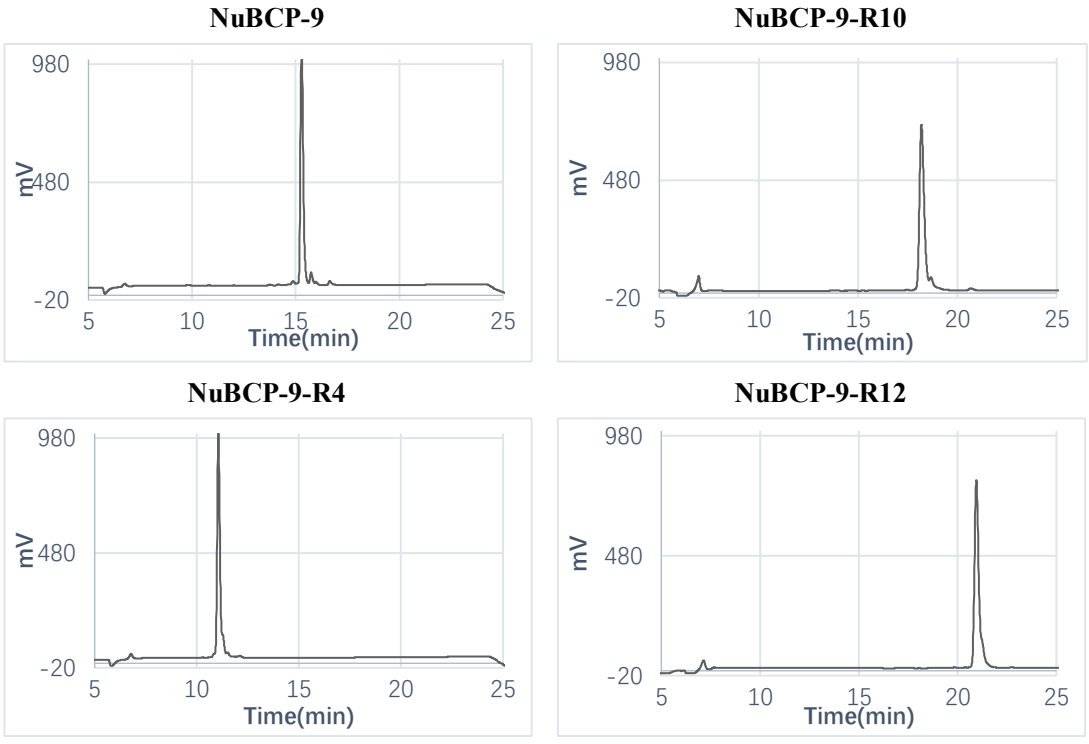

NuBCP-9-R6

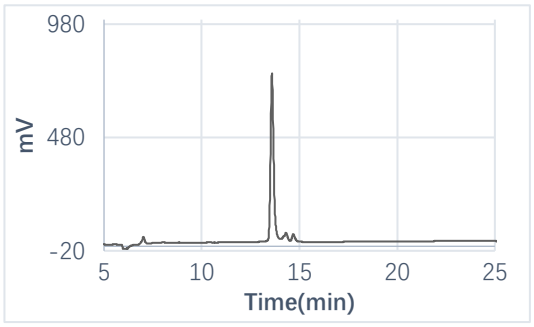

NuBCP-9-R14

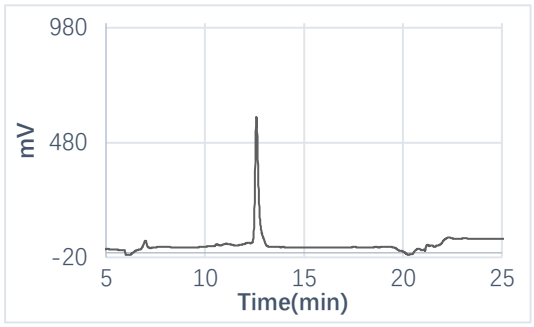

NuBCP-9-R8

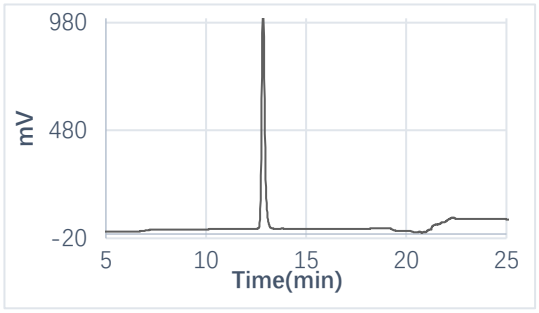

NuBCP-9-GX-R8

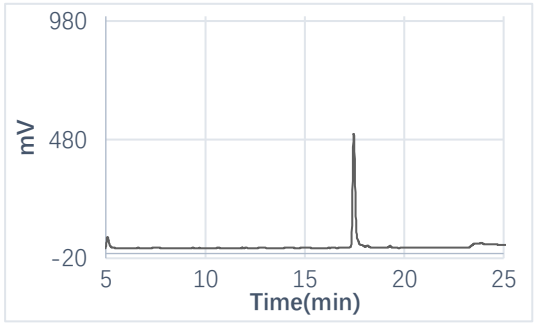

R6

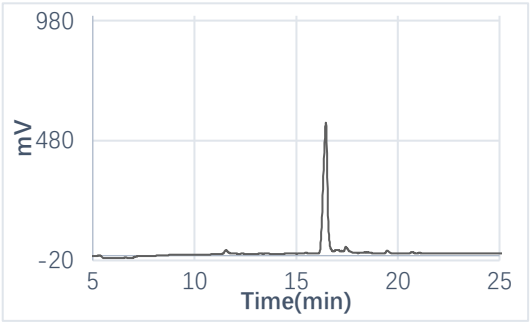

R14

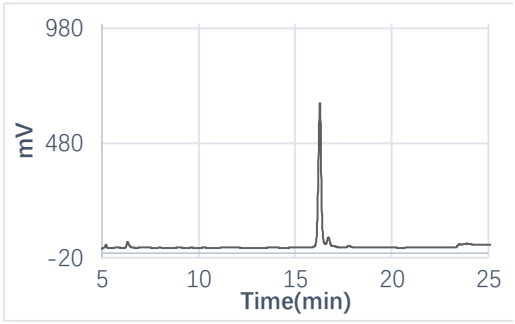

R8

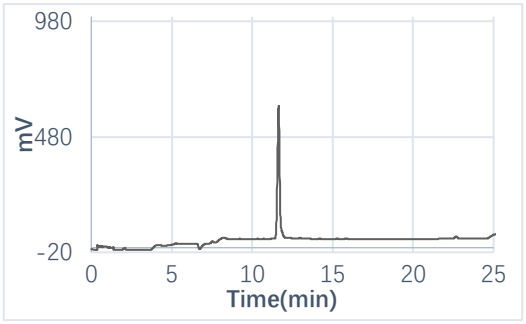

FA-R8

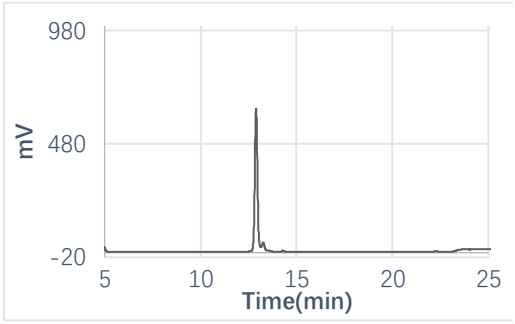

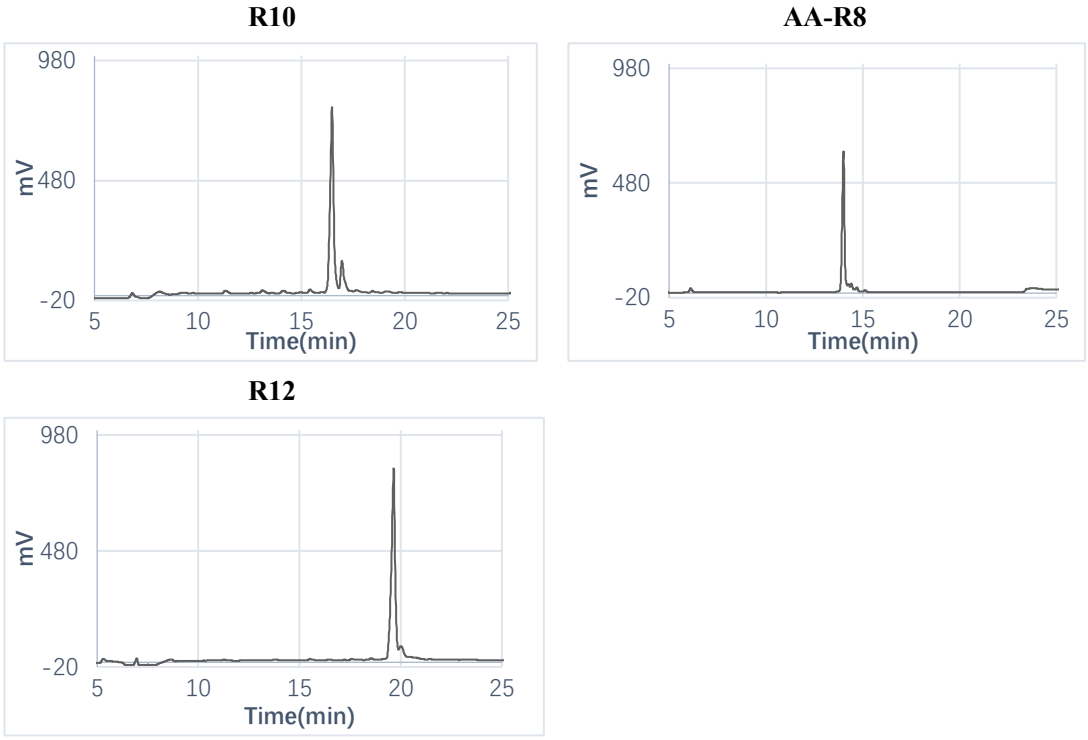

Fig.2 HPLC data about purity of synthesized peptides.

Tab. 2 Molecular weight of synthesized peptides that observed under MALDI-TOF-MS.

	Observed molecular weight (g/mol)	Theoretical molecular weight (g/mol)
NuBCP-9	1262.22	1260.48
NuBCP-9-R4	2058.54	2056.39
NuBCP-9-R6	2371.09	2368.76
NuBCP-9-R8	2683.69	2681.14
NuBCP-9-R10	2996.44	2993.51
NuBCP-9-R12	3306.75	3305.89
NuBCP-9-R14	3619.38	3618.26
R6	1157.99	1156.39
R8	1470.60	1468.77
R10	1783.20	1781.14
R12	2096.81	2093.52
R14	2410.76	2405.89
NuBCP-9-GX-R8	2684.87	2680.19
FA-R8	2641.95	2638.11
AA-R8	2566.96	2562.01

3.2. Fluorescence labelling of peptides

Thiol-maleimide reaction between sulfhydryl group of cysteine and maleimide is the most popular way to label the peptides with fluorescence[39,40] (Fig.3A). In the pH range of 6.5 to 7.5, maleimide can reaction with sulfhydryl groups rapidly and specifically. In pH 7.0, the reaction of maleimide with sulfhydryl groups proceeded 1,000 times greater than its reaction with amines[41]. In relatively high pH, cross-reaction with amino groups may result in complex product mixtures. Sufficient free sulfhydryl groups are essential for this conjugating, while in aqueous solution the sulfhydryl group of cysteine may be easily oxidized to form disulfide linkages[42]. Thus, disulfide reductants are recommended to be used for reverting disulfide to free sulfhydryl groups before labelling step, such as dithiothreitol (DTT) and TCEP[43]. While many articles and manual guide reported TCEP (< 20 mM) rarely competed with the thiol groups of cysteine in subsequent labelling reaction[44], I discovered this reductant reduced the labelling efficiency (Fig.3B). Thus, the disulfide reductant should be removed or eliminated before labelling reaction. Removing method, such as dialysis, may require deoxygenated conditions for keeping free sulfhydryl groups, thus selectively oxidizing excess TCEP·HCl in reaction mixture is preferred for diminishing this side reactions. 4-azidobenzoic acid (4-ABA) has been proved to selectively oxidize phosphine for improving efficiency of cysteine-maleimide conjugation (Fig.3C)[45]. Here, I studied the influence of reaction pH, dose of TCEP and 4-ABA for optimizing the conditions of labelling reaction.

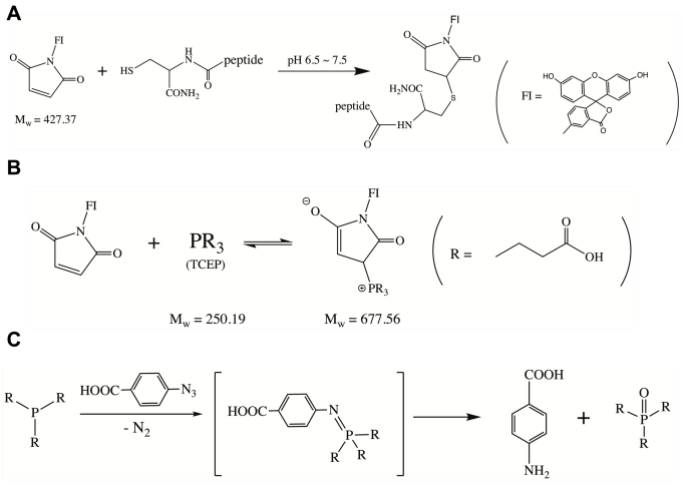

Fig.3 Reactions involved in fluorescein labeling experiment.

(A) Thiol-maleimide reaction between cysteine contained peptides and fluorescein-5-maleimide
(B) Possible reaction of TCEP with fluorescein-5-maleimide in aqueous buffers
(C) Oxidation of TCEP with 4-azidobenzoic acid

3.2.1. The influence of reaction pH on the labelling reaction

In Fig. 4, peak 2 was thought as the peak of target product and peak groups 1 were by-products. With increase of pH, the ratio of peak1/peak2 was increased. Therefore, the reaction pH should be carefully controlled under 7.0.

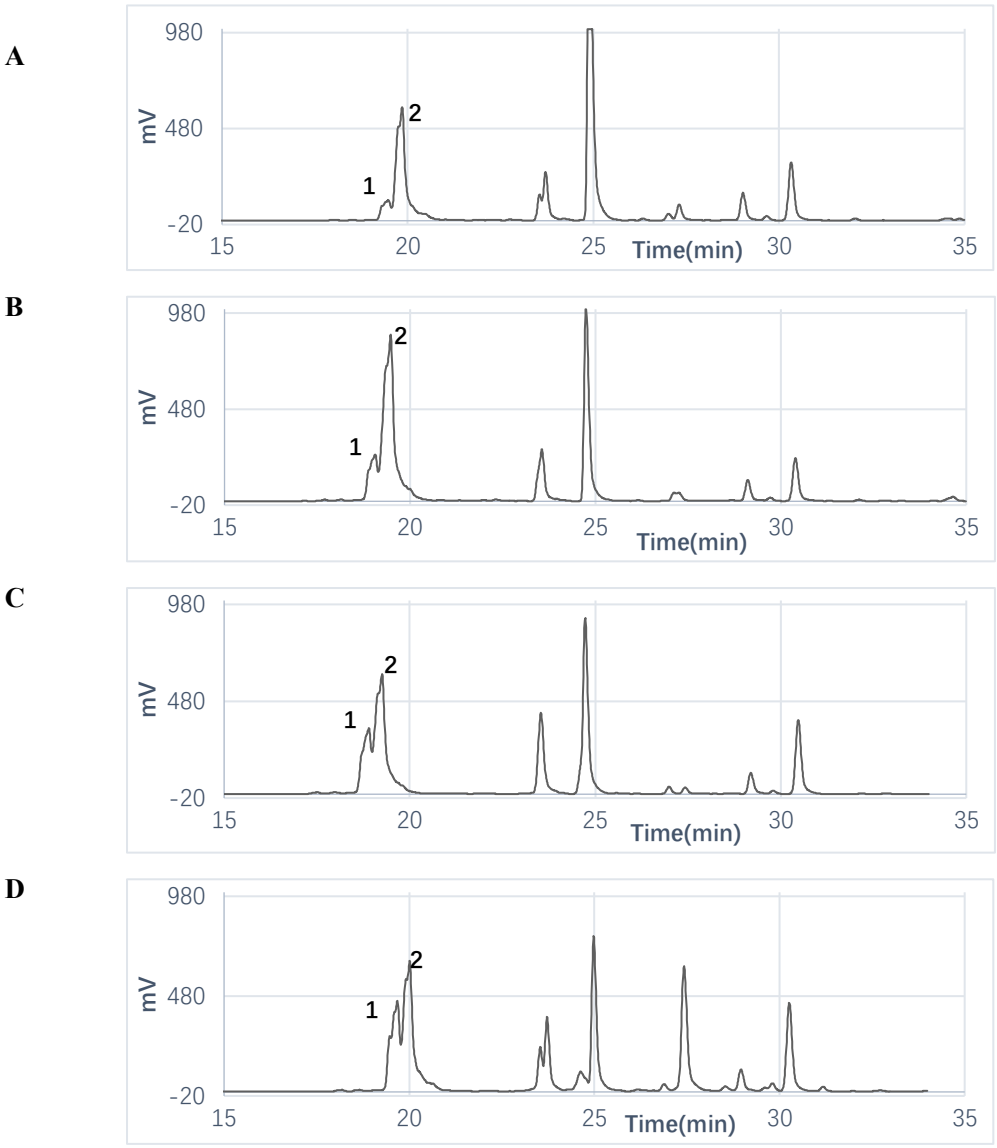

Fig.4 HPLC data about the influence of reaction pH on the labelling reaction.
（A） pH 6.8 (B) pH 7.0 (C) pH 7.3 (D) pH 7.6

3.2.2. The influence of TCEP·HCl on the labelling reaction

In Fig. 5, peak 1 was thought as the peak of target product. Without reductant

TCEP·HCl, little peptides were reacted with F5M. The labelling reaction was proceeded with higher molar ratio of TCEP/peptide. However, the products of peak 2 was proved as by-product from alkylation reaction (Fig.3B) between TCEP and F5M (mass of product: 678.68, observed in MALDI-TOF-MS) and the amount was also increased with higher molar ratio of TCEP/peptide. Such competed reaction should be eliminated for higher yield of target peptide product.

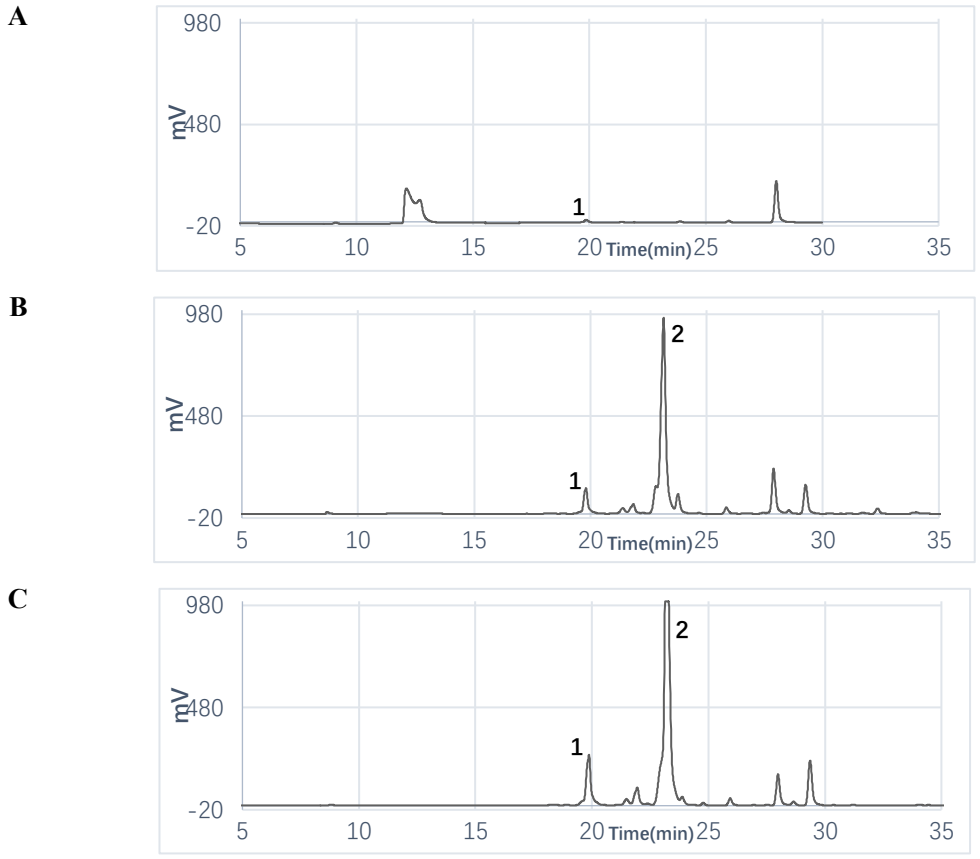

Fig. 5 HPLC data about the influence of TCEP on the labelling reaction.
(A) without TCEP (B) with 2 equiv. TCEP (C) with 5 equiv. TCEP

3.2.3. The influence of 4-ABA on the labelling reaction

For eliminating the side reaction of F5M with TCEP, 4-ABA was used to selectively oxidize excess TCEP in reaction mixture before coupling reaction of F5M with peptides[45].

From Fig.6, simple mixing reaction mixture with 10 equiv. 4-ABA for 15 min significantly diminished the reaction between F5M and TCEP during labelling step,

promoted efficiency of labelling reaction.

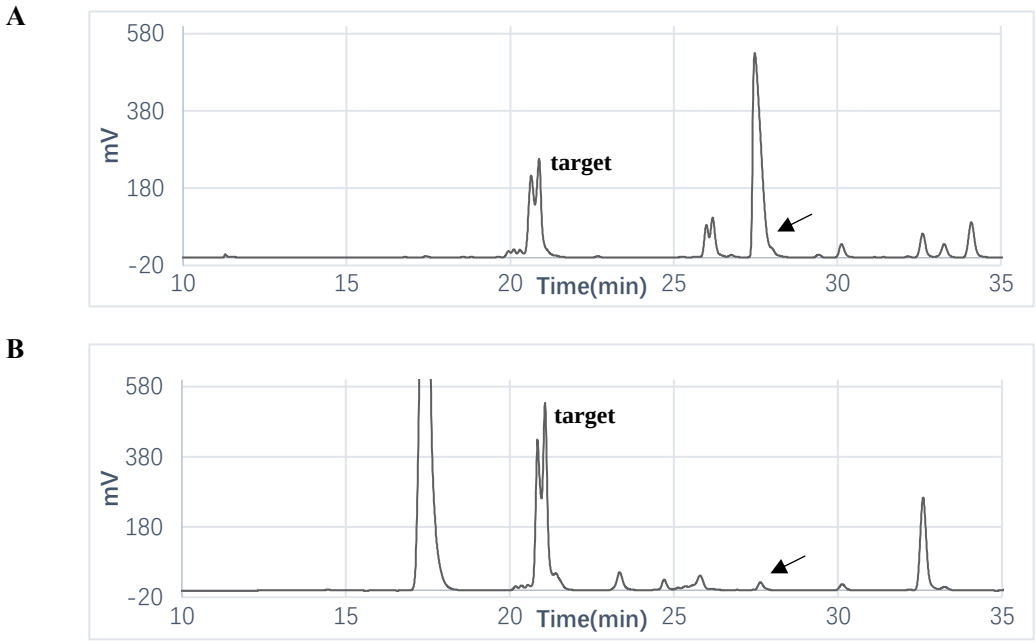

Fig. 6 HPLC data about the influence of 4-ABA on the labelling reaction.
(A) without 4-ABA (B) with 10 equiv. 4-ABA, arrow indicated side reaction of F5M with TCEP

3.2.4. Reaction, purification and structure identification of fluorescein labelled peptide

Through the optimized reaction protocol, the peptides were labelled with F5M. All the labelled peptides obtained over 90% purity after RP-HPLC purification (Fig.7). Besides, the molecular weight that observed under MALDI-TOF-MS was similar with the calculated value of each peptides (Tab.3).

Tab. 3 Molecular weight of fluorescein labelled peptides that observed under MALDI-TOF-MS.

	Observed molecular weight (g/mol)	Theoretical molecular weight (g/mol)
NuBCP-9-FI	1691.68	1687.85
NuBCP-9-R4-FI	2489.54	2483.76
NuBCP-9-R6-FI	2800.95	2796.13
NuBCP-9-R8-FI	3114.13	3108.51
NuBCP-9-R10-FI	3427.55	3420.88
NuBCP-9-R12-FI	3739.36	3733.26
NuBCP-9-R14-FI	4053.30	4045.63
R6-FI	1587.51	1583.76
R8-FI	1900.26	1896.14

R10-FI	2212.74	2208.51
R12-FI	2526.58	2520.89
R14-FI	2839.29	2833.26
FA-R8-FI	3072.53	3065.48
AA-R8-FI	2995.18	2989.38

R6-FI

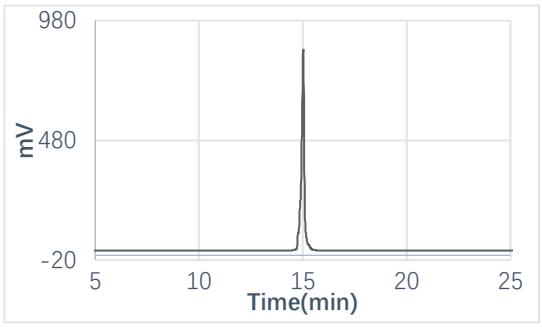

R14-FI

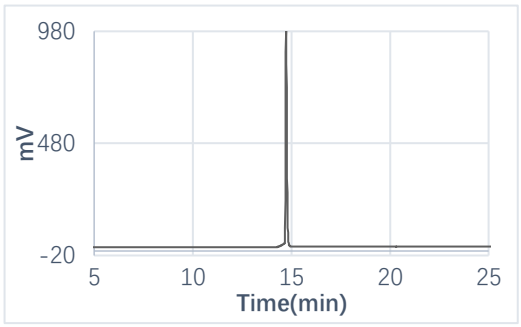

R8-FI

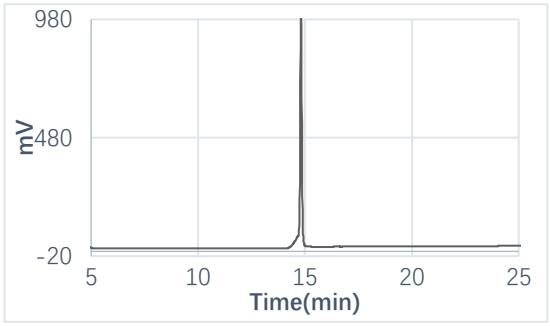

NuBCP-9-FI

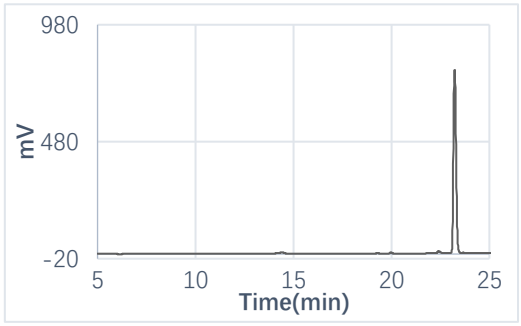

R10-FI

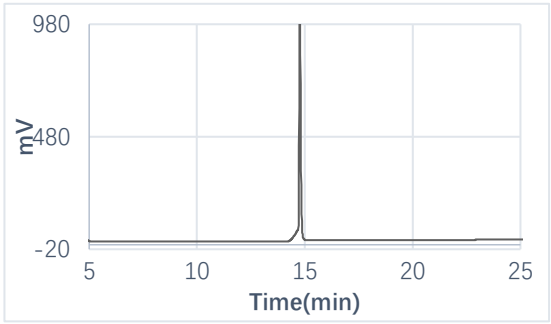

FA-R8-FI

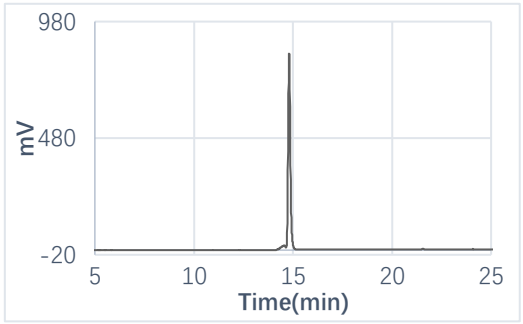

R12-FI

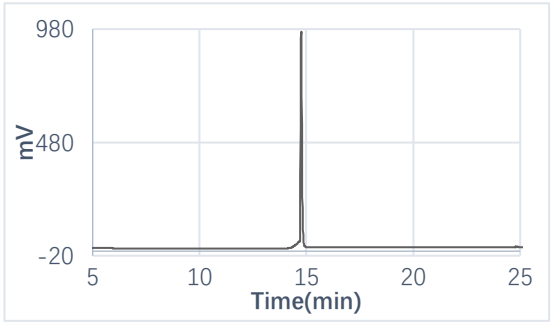

AA-R8-FI

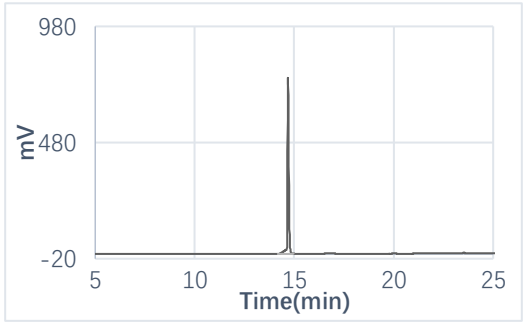

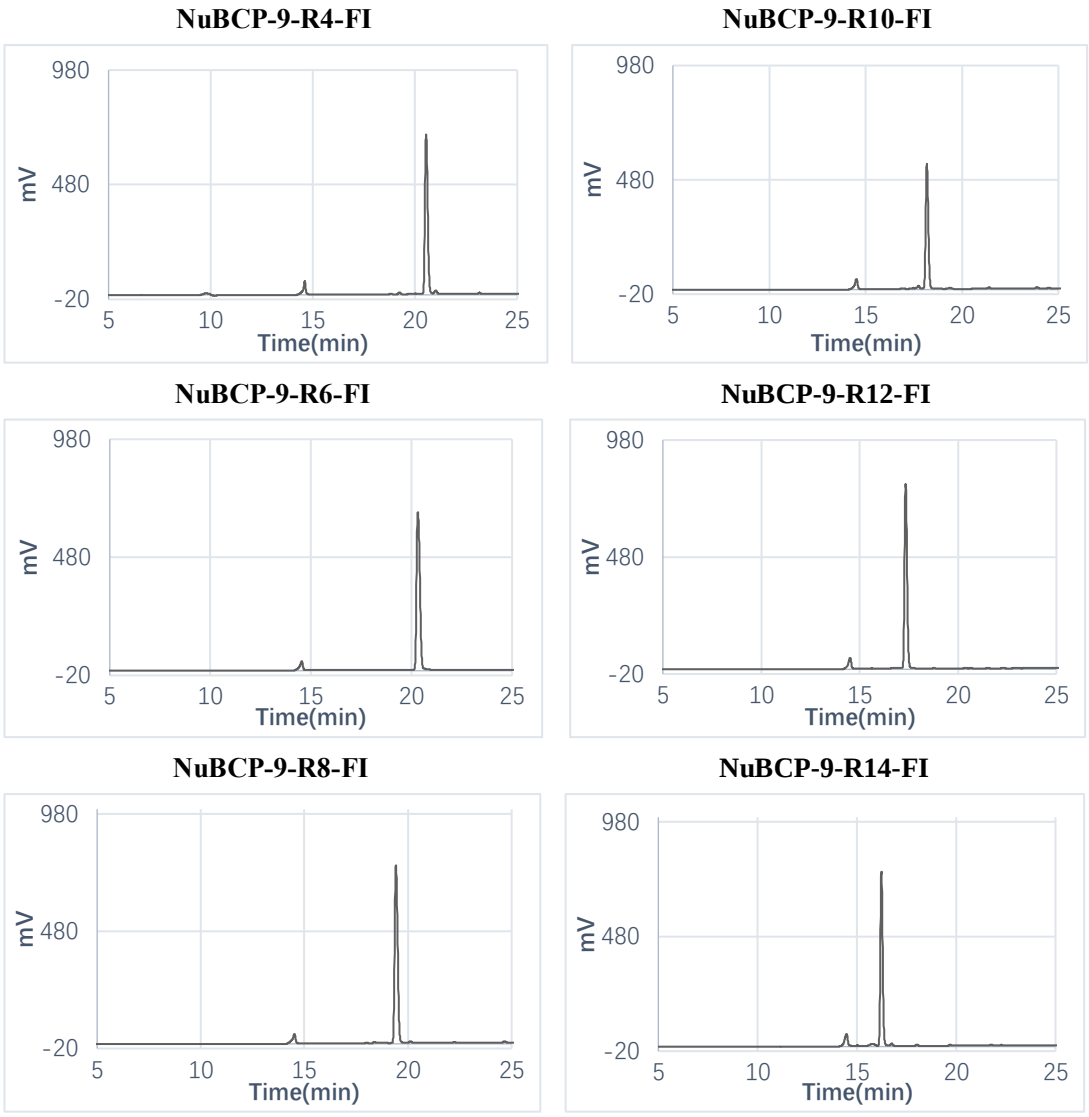

Fig 7. HPLC data about purity of fluorescein labelled peptides.

3.3. Cellular uptake of Rn and NuBCP-9-Rn conjugates

3.3.1. Influence factors on cellular uptake of peptides (heparin washing step, incubation time and treatment concentration)

Suitable conditions should be used for evaluating the cellular uptake of Rn. It has been proved that fixation of cells may cause artifacts on cellular distribution. Additionally, in the absence of trypsinization and heparin washing the uptake fluorescence intensity may be overestimated with membrane binding portion[46,47]. The electrostatic interaction between arginine-rich cell penetrating peptides and membrane associated proteoglycans such as heparan sulfate has been proved to play an important role in activating macropinocytotis[48]. Therefore, the washing step with heparin

contained PBS are commonly used way for removing membrane binding peptides.

In this part, I plan to prove the importance of heparin washing step and decide the suitable co-incubation duration and treatment dose for evaluating the cellular uptake of Rn and NuBCP-9-Rn conjugates.

From the results in Fig.8, using heparin supplemented PBS to wash the harvest cells significantly decreased the detected fluorescence intensity of R8 compare with the PBS washing group. The PBS washing group had broader distribution of fluorescence intensity of R8 than heparin washing group.

In Fig.9, when incubated cells with 2 μM R8 contained medium for different duration, 1h and 2 h treatment showed mildly increased but not significant uptake level of peptides than 30min treatment. While it had a progressive decline in uptake of peptides from 2h to 24h treatment.

After incubation with R8 or NuBCP-9-R8 conjugate with various dose, the uptake level of R8 exhibited a mild increase from 2 to 10 μM. Meanwhile, it showed a sharp increased uptake of NuBCP-9-R8 conjugate at same range. The uptake of NuBCP-9-R8 conjugate was found to be significantly higher than the uptake of R8 when the peptide dose was above 4 μM (Fig.10).

Thus, heparin washing step, 30 min co-incubation duration, 2 μM and 10 μM treatment concentration were selected as the basic condition for evaluating the cellular uptake of Rn and NuBCP-9-Rn conjugates in the future work.

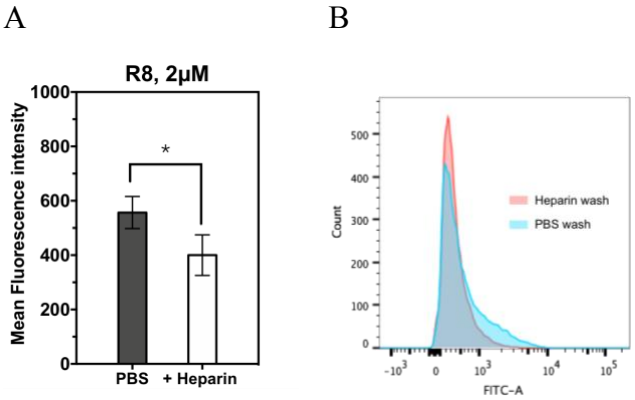

Fig.8 Influence of heparin washing step on the cellular uptake of R8.
(A) MDA-MB-231 cells were incubated with 2 μM fluorescein labeled R8 for 30 min at 37 ℃. After washing the harvested cells twice with PBS or 20 U/mL heparin supplemented PBS, the uptake level

was quantified by flow cytometry. Error value represents the mean ± SD from triplicate experiments (ANOVA, t test, $^{*}p < 0.05$). (B) The comparison files of FACS was showed. 10,000 counts were taken for each sample.

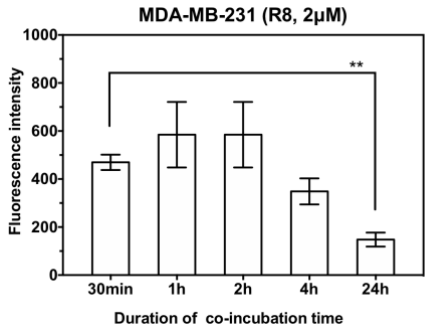

Fig.9 Influence of co-incubation duration on the cellular uptake of R8.
MDA-MB-231 cells were incubated with 2 μM fluorescein labeled R8 for 30 min, 1 , 2 , 4 or 24 h at 37 ℃. The uptake level was quantified by flow cytometry. Error value represents the mean ± SD from triplicate experiments (ANOVA, Dunnett's test, compare with 30min treatment group, $^{**}p < 0.01$). 10,000 counts were taken for each sample.

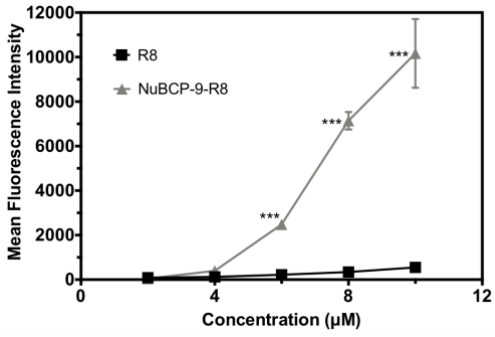

Fig.10 Influence of treatment concentration on the cellular uptake of R8 and NuBCP-9-R8 conjugate.
MDA-MB-231 cells were incubated with 2 - 10 μM fluorescein labeled R8 or NuBCP-9-R8 conjugate for 30 min at 37 ℃. The uptake level was quantified by flow cytometry. Error value represents the mean ± SD from triplicate experiments (ANOVA, Bonferroni test, $^{***}p < 0.001$).

3.3.2. Cellular uptake of Rn and NuBCP-9-Rn conjugates

After making the basic protocol, I evaluated the cellular uptake level of Rn and NuBCP-9-Rn (n=0, 6, 8, 10, 12 and 14) conjugates at 2 μM and 10 μM. At 2 μM, R12 showed the highest uptake level among Rn (Fig. 11A). There was little difference of uptake of Rn with or without conjugating with NuBCP-9 at 2 μM. NuBCP-9-R10 and NuBCP-9-R12 conjugates showed higher uptake levels than any other NuBCP-9-Rn conjugates. At 10 μM (Fig. 11B), Rn showed a similar uptake efficiency at 2 μM. On the contrary, the uptake of NuBCP-9-Rn conjugates at 10 μM was significantly

enhanced compared to the uptake of Rn without NuBCP-9 conjugation. NuBCP-9-R10 conjugate showed the highest uptake level at 10 μM, and it was about 13 times higher than R10 and 9 times than R12.

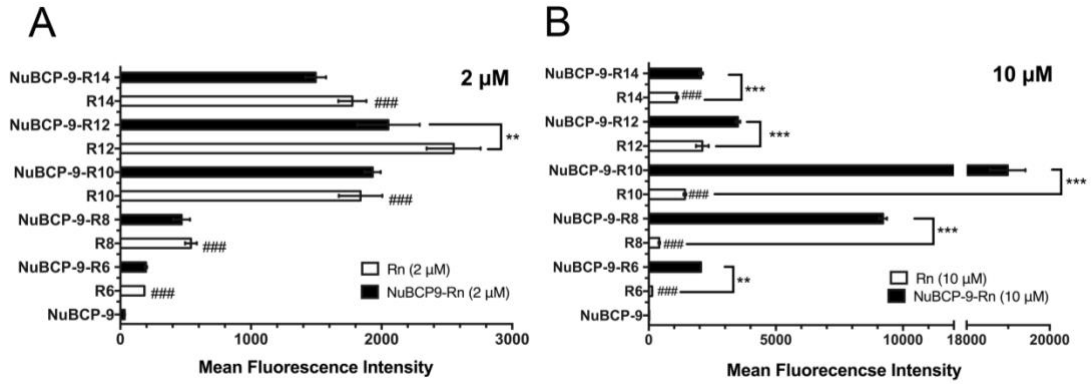

Fig.11 Cellular uptake Rn and NuBCP-9-Rn conjugates in MDA-MB-231 cells.
MDA-MB-231 cells were incubated with (A) 2 or (B) 10 μM fluorescein labeled Rn or NuBCP-9-Rn (n = 0, 6, 8, 10, 12 and 14) conjugates for 30 min at 37 ℃. The uptake level was quantified by flow cytometry. Error value represents the mean ± SD from triplicate experiments. 10,000 counts were taken for each sample. (ANOVA, Bonferroni test, * Significant difference between Rn and NuBCP-9-Rn conjugates, ** $p < 0.01$, *** $p < 0.001$, $^{\#}$ Significant difference between R12 and each treatment with Rn, $^{\#\#\#}$ $p < 0.001$).

3.3.3. Subcellular distribution of Rn and NuBCP-9-Rn conjugates

For exploring the cellular distribution of Rn and NuBCP-9-Rn conjugates, the living cells which had been treated with 2 or 10 μM fluorescein labelled peptides were observed under CLSM. Trypan blue is impermeable to the cell membrane and has ability to quench the extracellular fluorescent labels[49,50], thus it was added into culture medium before observing procedures. In this research, a cell-permeant nuclear counterstain, Hoechst 33342 was used for staining nuclear instead of the commonly used reagent DAPI, which cannot permeate to live cell membrane. At 2 μM, Rn and NuBCP-9-Rn (n = 8, 10, 12, and 14) conjugates were internalized into punctate vesicles as shown in Fig. 12A. At 10 μM, R8 was mainly located vesicular structures, as can be seen in Fig. 12B. However, R10, R12, R14, and all NuBCP-9-Rn (n = 6, 8, 10, 12, and 14) conjugates were visualized as diffusely distributed in the cytoplasm. NuBCP-9-R8, and NuBCP-9-R10 conjugates showed significantly enhanced cytoplasmic labelling compared to NuBCP-9-R12 and NuBCP-9-R14 conjugates, and brighter staining of the

nucleus by the peptides was observed in some cells. The NuBCP-9-R10 conjugate exhibited the strongest cellular fluorescence signal. Those are in agreement with the flow cytometry results depicted in Fig. 11.

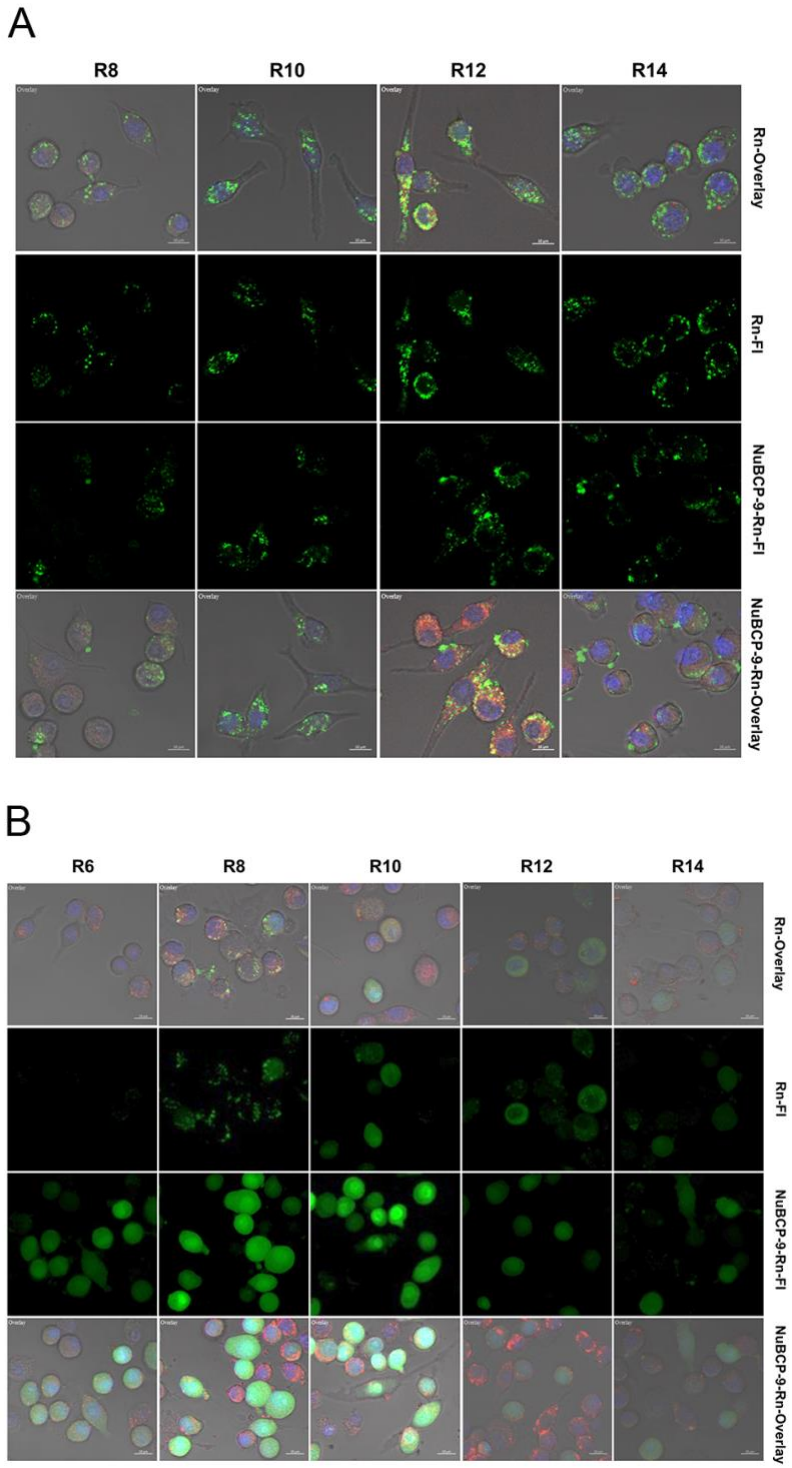

Fig.12 Subcellular distribution of Rn and NuBCP-9-Rn conjugates.
MDA-MB-231 cells were incubated with (A) 2 or (B) 10 μM fluorescein labelled Rn and NuBCP-9-Rn (n = 6, 8, 10, 12 and 14) conjugates (green) for 30 min at 37℃ and observed by CLSM.

Lysotracker Red (red) and Hoechst 33342 (blue) were also added in peptides contained medium for lysosomes and nuclei staining, respectively. Scale bars: 10 μm.

3.4. Investigation of uptake mechanism of NuBCP-9-R8 conjugate by amino acid replacement of NuBCP-9

To investigate the presence of a hydrophobicity switch with respect to the uptake of NuBCP-9-R8 conjugate in MDA-MB-231 cells, I synthesized NuBCP-9-R8-derived conjugates (FA-R8 and AA-R8) with differ hydrophobicity resulting from a molecular change at their distal ends (Tab. 1). FA-R8 conjugate replaced leucine with alanine at C-terminus of NuBCP-9-R8 conjugate. At 10 μM, there was an approximately 300% decrease in the uptake of FA-R8 conjugate relative to NuBCP-9-R8 conjugate. AA-R8 conjugate replaced phenylalanine with alanine at N-terminus of FA-R8 conjugate. There was an approximately 700% decrease in the uptake of this modified conjugate at 10 μM relative to FA-R8 conjugate (Fig. 13B). The NuBCP-9- R8-derived conjugate with low hydrophobicity at both its distal positions, AA-R8 conjugate, in fact had an uptake level similar to that of unconjugated R8. At 2 μM, all the hydrophobic replacement showed little influence on the cellular uptake of R8 (Fig. 13A).

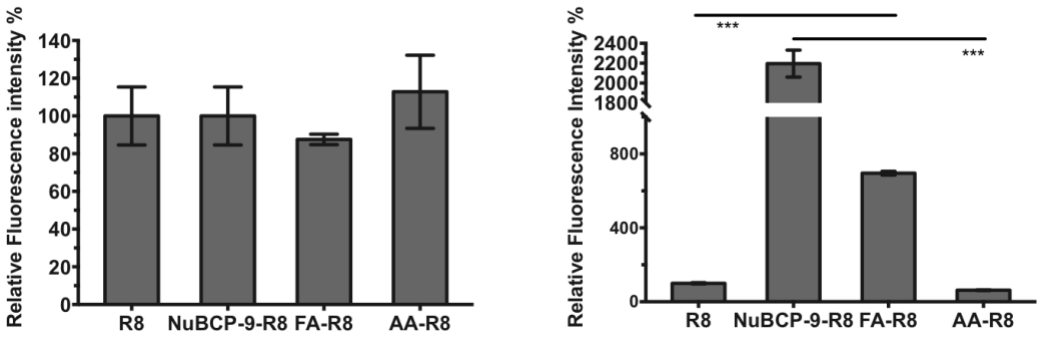

Fig.13 Uptake efficiency of conjugates with modified hydrophobicity.
MDA-MB-231 cells were incubated with (A) 2 or (B) 10 μM fluorescein labeled R8, NuBCP-9-R8 conjugate, FA- R8 conjugate, and AA-R8 conjugate for 30 min at 37℃. The uptake level was quantified by flow cytometry. Each value represents the mean ± SD from triplicate experiments. (ANOVA, Bonferroni test, *** $p < 0.001$). 10,000 counts were measured for each sample.

3.5. Uptake pathways of Rn and NuBCP-9-Rn conjugates

For understanding the uptake pathways of Rn and NuBCP-9-Rn conjugates, I focused on three typical pathways: clathrin-mediated endocytosis, caveolae-mediated

endocytosis and macropinocytosis. Chlorpromazine (CPZ), genistein and EIPA were used as inhibitors of each uptake pathways in this part, respectively[21,51,52]. Additionally, the uptake of CPPs was also influenced by temperature[39,53]. The uptake of Rn and NuBCP-9-Rn conjugates under lower temperature was also determined.

3.5.1. Influence of treatment dose of uptake inhibitors on cell survival

The cytotoxicity of three uptake inhibitors needs preliminary check[52] for finding suitable treatment dose in MDA-MB-231 cells. The cell viabilities of MDA-MB-231 cells after 1h co-incubation with each uptake inhibitors were preliminarily evaluated with WST-8 assay kits. From the results in Fig. 14, the cell viability was decreased when the treatment concentration of CPZ or EIPA increased. The maximum acceptable concentration of CPZ and EIPA was 50 μM and 100 μM, respectively. On the other hand, even 300 μM genistein was harmless to MDA-MB-231 cells. Thus, 50 μM, 100 μM and 200 μM was selected as the dose of CPZ, EIPA and genistein based on the previous study, respectively[54–56].

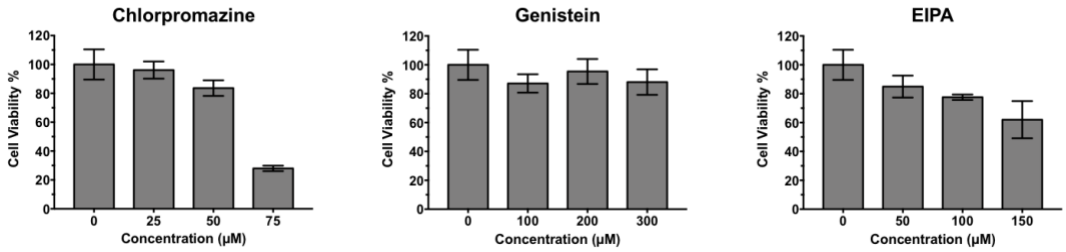

Fig. 14 Cytotoxicity of uptake inhibitors in MDA-MB-231 cells.
Viability of MDA-MB-231 cells following a 1 h incubation with indicated concentration of chlorpromazine, genistein or EIPA. Each value represents the mean ± SD from triplicate experiments.

3.5.2. Influence of uptake inhibitors on cellular uptake of Rn and NuBCP-9-Rn conjugates

Uptake level of Rn and NuBCP-9-Rn (n= 8, 10, 12 and 14) conjugates in the presence of CPZ, genistein or EIPA were analyzed under flow cytometer. From the results in Fig. 15, in the presence of CPZ or EIPA, Rn and NuBCP-9-Rn conjugates entry were suppressed significantly in MDA-MB-231 cells at 2 μM and 10 μM.

Particularly, the inhibition rate was increased with 100 μM EIPA when concentration of peptides was switched from 2 μM (Fig.15A) to 10 μM (Fig.15B). Co-incubation with 200 μM genistein did not inhibited the uptake of all peptides at both two concentrations.

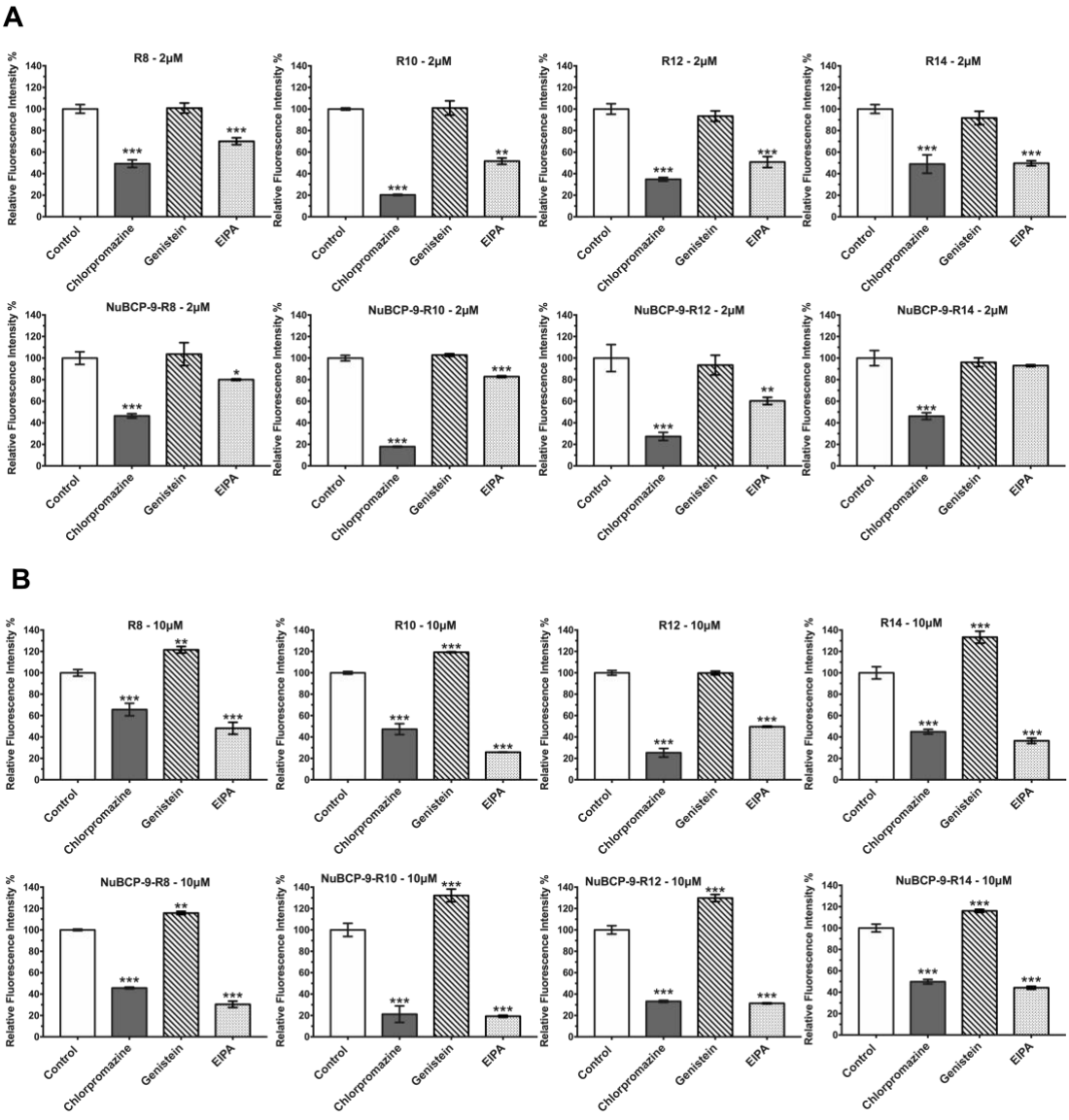

Fig.15 Influence of uptake inhibitors on cellular uptake of Rn and NuBCP-9-Rn conjugates.

MDA-MB-231 cells were incubated for 30 min with (A) 2 or (B) 10 μM fluorescein labeled Rn or NuBCP-9-Rn (n= 8, 10, 12 and 14) conjugates in the absence or presence of 50 μM CPZ, 200 μM genistein, or 100 μM EIPA, respectively. Uptake of peptides was quantified by flow cytometry. The results are expressed as a percent of the fluorescence measured in the absence of inhibitors. Each value represents the mean ± SD from triplicate experiments. 10,000 counts were taken for each sample. (ANOVA, Dunnett's test, * $p < 0.05$, ** $p < 0.01$, *** $p < 0.001$)

3.5.3. Influence of uptake inhibitors on cellular distribution of Rn and NuBCP-9-Rn conjugates

At concentrations of 2 or 10 μM (Fig. 16), when compared with control group (no inhibitors), the uptake level of peptides was suppressed under chlorpromazine or EIPA treatment. In addition, the subcellular distribution was changed, with staining in the nucleolus or diffuse cytoplasmic staining becoming much dimmer than that seen in the control group. Cells co-incubated with peptides and genistein showed no changes in cellular distribution of the peptides or fluorescence staining intensity when compared with the control group cells.

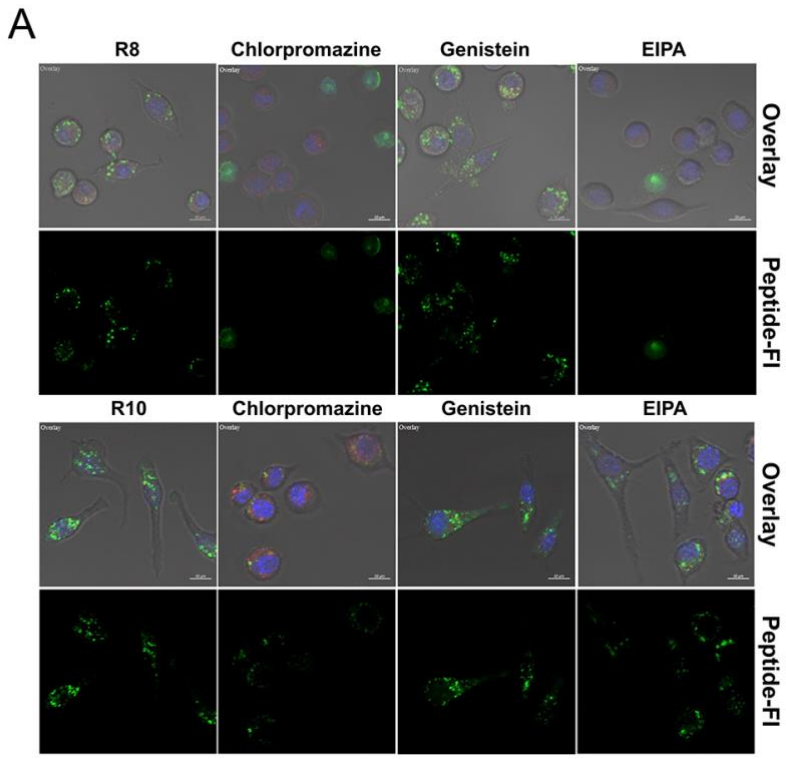

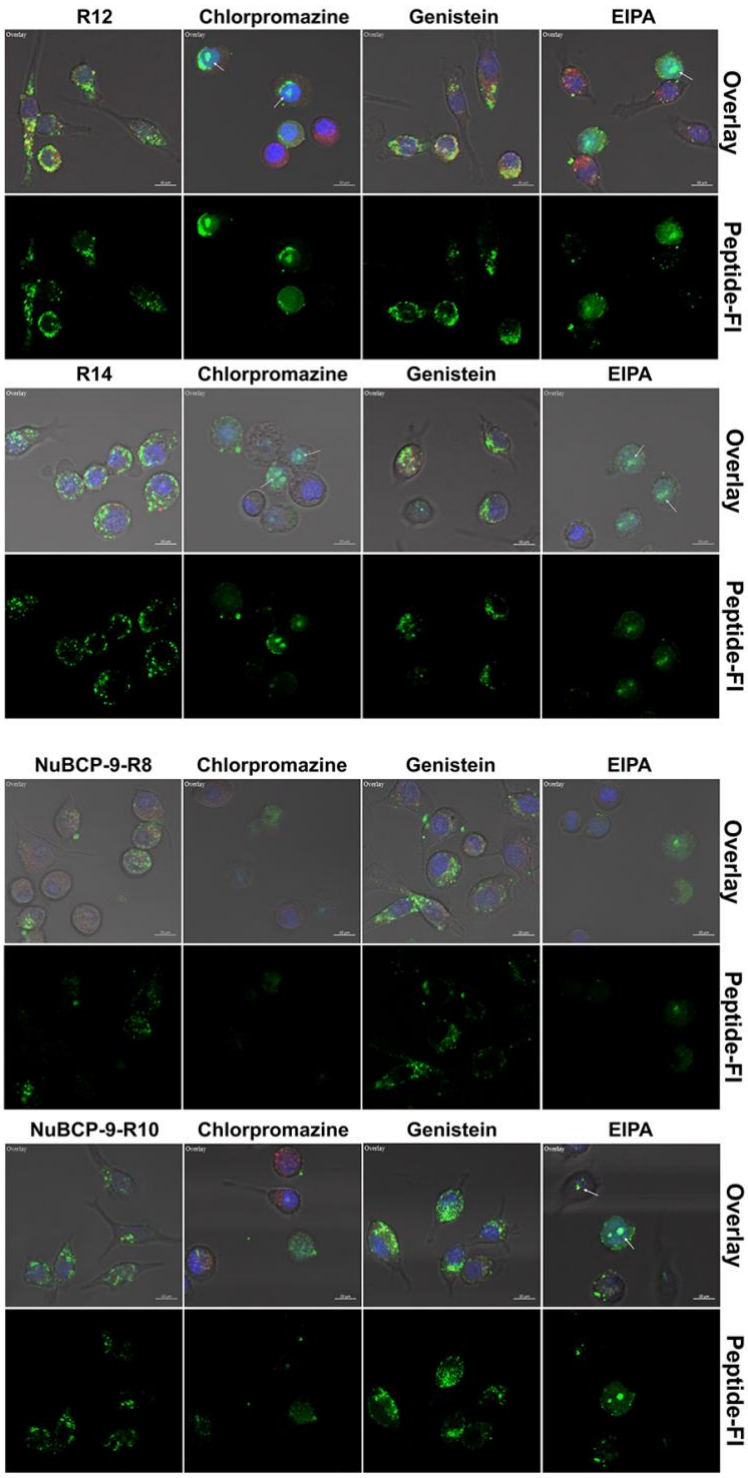
R12
Chlorpromazine
Genistein
EIPA
Overlay
Peptide-FI
R14
Chlorpromazine
Genistein
EIPA
Overlay
Peptide-FI
NuBCP-9-R8
Chlorpromazine
Genistein
EIPA
Overlay
Peptide-FI
NuBCP-9-R10
Chlorpromazine
Genistein
EIPA
Overlay
Peptide-FI

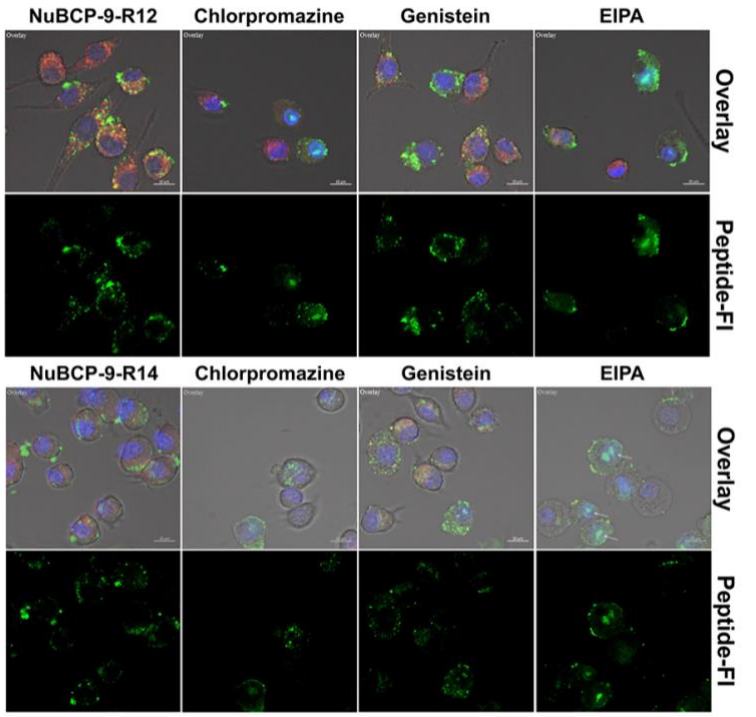
NuBCP-9-R12
Chlorpromazine
Genistein
EIPA
Overlay
Peptide-FI
NuBCP-9-R14
Chlorpromazine
Genistein
EIPA
Overlay
Peptide-FI

B

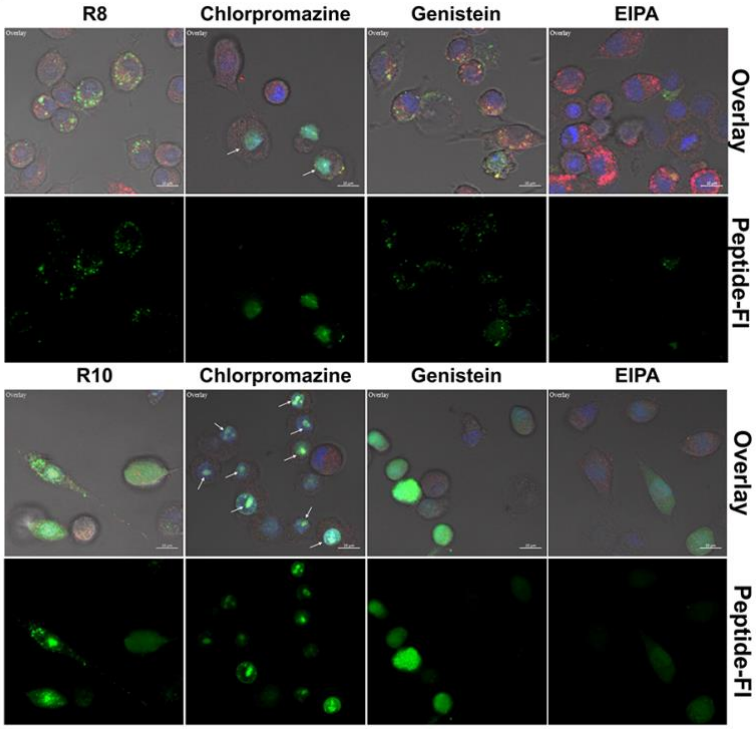
R8
Chlorpromazine
Genistein
EIPA
Overlay
Peptide-FI
R10
Chlorpromazine
Genistein
EIPA
Overlay
Peptide-FI

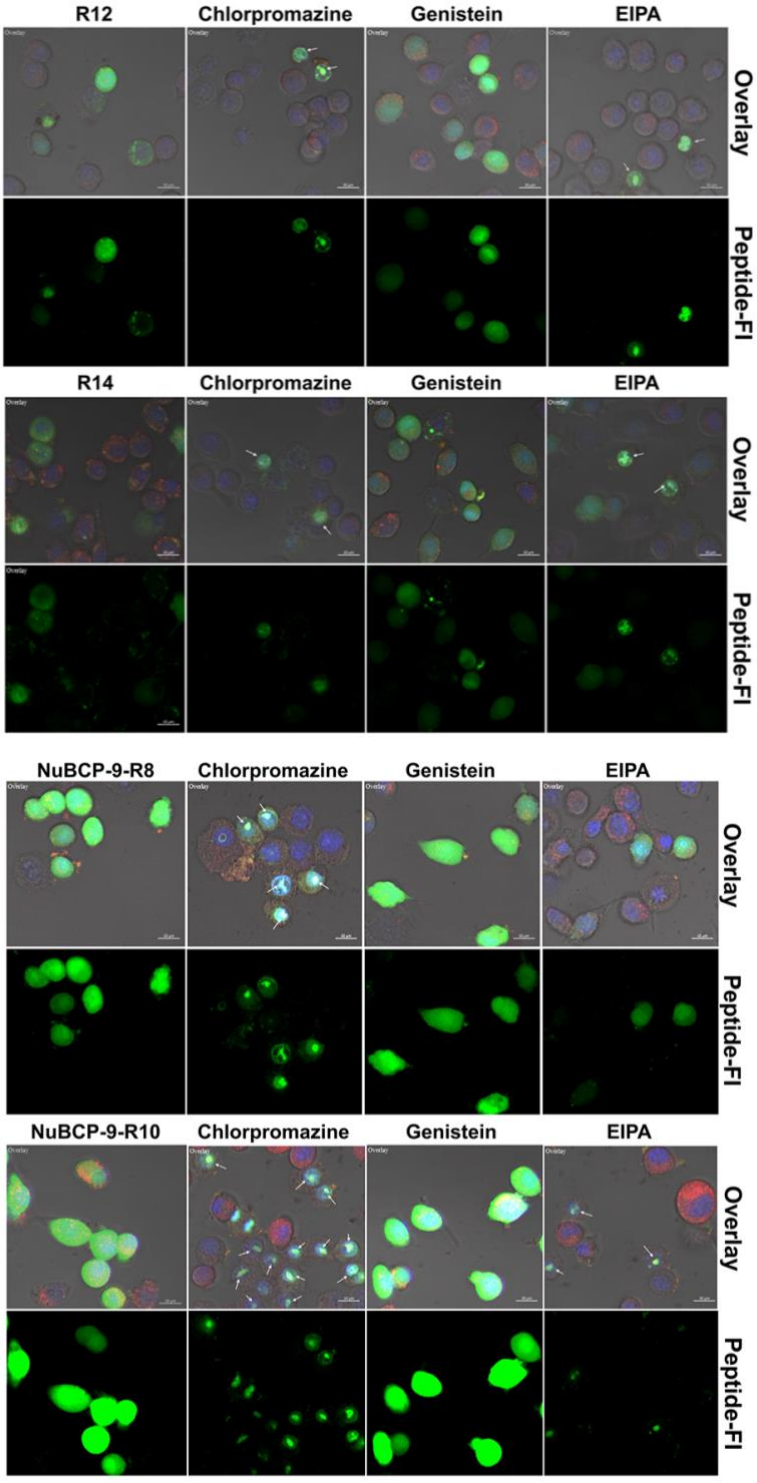
R12
Chlorpromazine
Genistein
EIPA
Overlay
Peptide-FI
R14
Chlorpromazine
Genistein
EIPA
Overlay
Peptide-FI
NuBCP-9-R8
Chlorpromazine
Genistein
EIPA
Overlay
Peptide-FI
NuBCP-9-R10
Chlorpromazine
Genistein
EIPA
Overlay
Peptide-FI

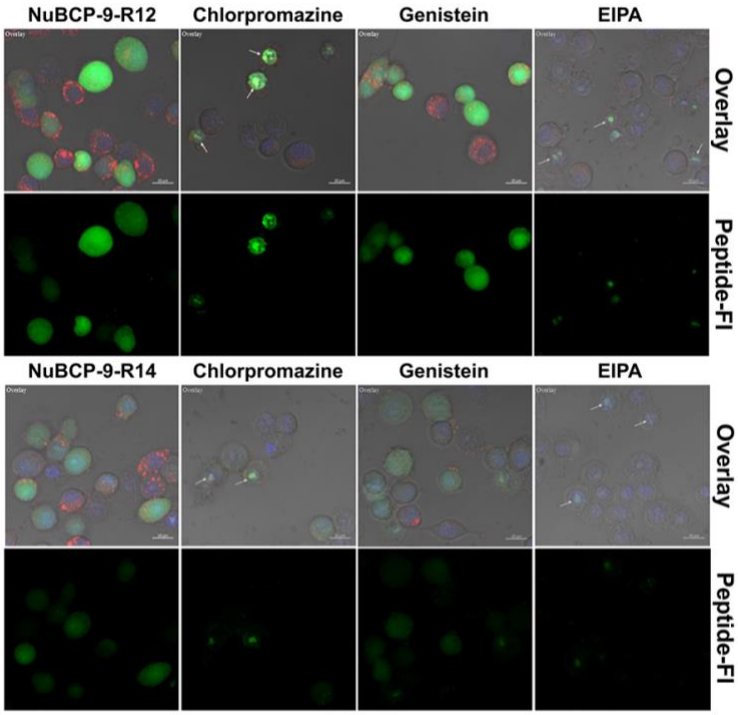

Fig.16 Influence of uptake inhibitors on cellular distribution of Rn and NuBCP-9-Rn conjugates. The cellular distribution of (A) 2 or (B) 10 μM fluorescein labeled Rn or NuBCP-9-Rn (n =8, 10, 12, and 14) conjugates in the absence or presence of 50 μM chlorpromazine, 200 μM genistein, or 100 μM EIPA, respectively. Uptake of peptides (green) were analyzed by confocal microscopy. Lysotracker Red (red) and Hoechst 33342 (blue) were also added in peptides contained medium for lysosomes and nuclei staining, respectively. Arrows indicate peptide labelling of nucleolus. Scale bars: 10 μm.

3.5.4. Influence of temperature on cellular uptake of Rn and NuBCP-9-Rn conjugates

MDA-MB-231 cells were treated under a lower temperature condition (4 ℃) to determine if the uptake of peptides was energy dependency. After pretreatment and incubation with peptides for 30 min at 4 ℃, the cellular uptake of peptides was partly inhibited for 2 μM and 10 μM (Fig.17), while the inhibition rate was diverse (Tab.4). 4 ℃ treatment led more inhibition on the uptake of NuBCP-9-Rn conjugates than Rn at both two concentrations.

Tab. 4 Inhibition rate on uptake of Rn and NuBCP-9-Rn (n = 8, 10, 12, 14) conjugates at 4 ℃.

Inhibition rate	Rn		NuBCP-9-Rn	
(%)	2 μM	10 μM	2 μM	10 μM
8	27.08 ± 1.03	31.61 ± 2.18	49.86 ± 4.12	73.29 ± 6.57
10	44.85 ± 2.59	25.70 ± 1.13	53.49 ± 0.73	76.82 ± 3.13
12	75.42 ± 0.83	60.70 ± 1.65	86.99 ± 1.00	38.15 ± 4.02
14	83.54 ± 0.50	35.75 ± 2.48	88.77 ± 0.31	42.34 ± 4.99

Each value represents the mean ± SD from triplicate experiments.

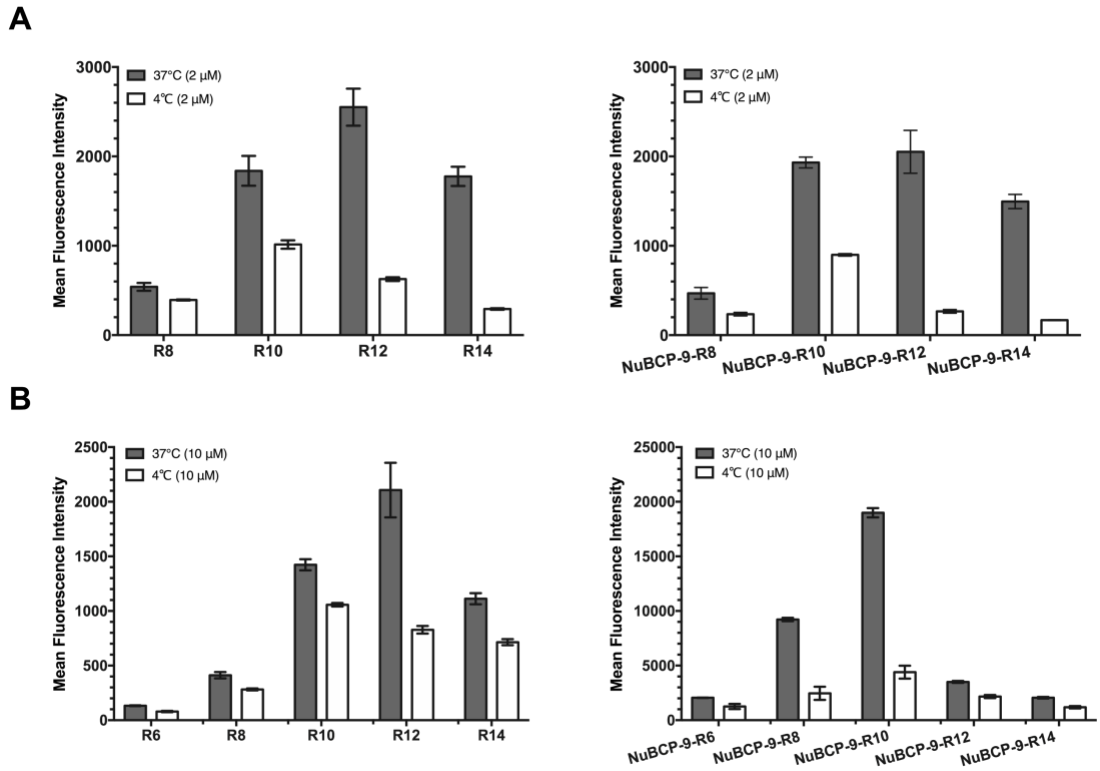

Fig.17 Influence of temperature on cellular uptake of Rn and NuBCP-9-Rn conjugates.

MDA-MB-231 cells were incubated with (A) 2 or (B) 10 μM fluorescein labelled Rn and NuBCP-9-Rn (n =6, 8, 10, 12 and 14) conjugates for 30 min at 4 ℃ prior to trypsin treatment and heparin washing, then peptide uptake was quantified by flow cytometry. The results are expressed as a percent of the fluorescence measured in the absence of inhibitors. Each value represents the mean ± SD from triplicate experiments. 10,000 counts were taken for each sample.

3.5.5. Influence of temperature on cellular distribution of Rn and NuBCP-9-Rn conjugates

After that the cellular distribution of peptides was observed under 4 ℃ treatment. Comparing with the view under 37 ℃ (Fig. 12), the internalization level of all peptides was significantly suppressed at 4 ℃ (Fig. 18). Unlike the punctate endosomal labelling

under 37 ℃, low temperature treatment led modest cytoplasmic diffuse labelling of peptides in MDA-MB-231 cells at 2 μM (Fig. 18A). Similar with the results with uptake inhibitors CPZ or EIPA (Fig.16), nucleolus staining was occurred in some cells (Fig.18).

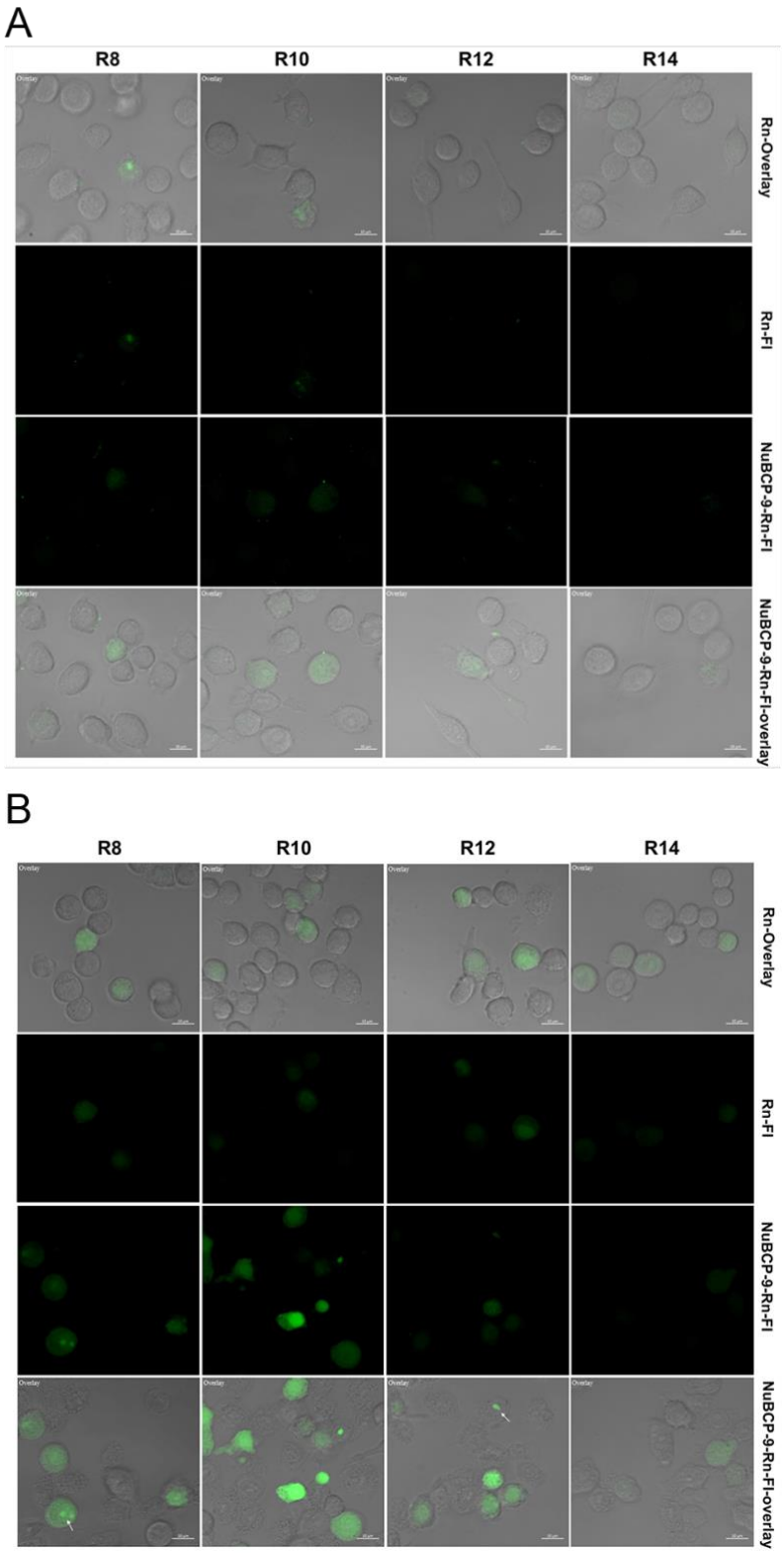

Fig.18 Influence of temperature on cellular distribution of Rn and NuBCP-9-Rn conjugates. MDA-MB-231 cells were incubated with (A) 2 or (B) 10 μM fluorescein labelled Rn and NuBCP-

9-Rn (n = 6, 8, 10, 12 and 14) conjugates (green) for 30 min at 4 ℃ and observed by CLSM. Arrows indicate peptide labelling of nucleolus. Scale bars: 10 μm.

4. Discussion

Oligoarginines, as a type of CPP, have been commonly utilized for intracellular delivery of therapeutic peptides because of the simple synthesis procedure and high uptake efficiency of conjugates[13]. NuBCP-9, a Bcl-2 targeting proapoptotic peptide, has been proven to have synergy with R8, and the resultant conjugate exhibited enhanced uptake efficiency while also inducing a degree of non-specific membrane disruption[31]. Although such an enhanced uptake effect has been seen with other CPPs after reverting the hydrophobicity of other cargo peptide, the degree of enhancement has generally relied on the intrinsic uptake efficiency of the CPPs used[25]. In the case of oligoarginines, uptake efficiency has been shown to be dependent on the number of arginines present in the oligomer[19]. Therefore, Rn of different lengths may perform differently in terms of uptake efficiency and non-specific cytotoxicity following conjugation with NuBCP-9. I first evaluated the uptake efficiency and cellular distribution of Rn before and after conjugation with NuBCP-9, to investigate how NuBCP-9 influences the uptake behavior of Rn of different lengths.

Without conjugating of Rn, NuBCP-9 was difficult to be delivered into cells, while NuBCP-9-Rn conjugates showed significant higher uptake (Fig.11), it suggests that Rn (n=8, 10, 12, and 14) may be the vectors to induce the uptake of NuBCP-9. The uptake levels of unconjugated Rn and NuBCP-9-Rn conjugates at 2 μM were slightly different (Fig. 11A), but uptake of NuBCP-9-Rn conjugates at 10 μM was significantly elevated compared to that of unconjugated Rn at the same concentration (Fig.11B). The uptake behavior of cationic CPPs including oligoarginines has been shown to demonstrate differing behavior above and below a concentration threshold in previous studies as well[57,58]. The uptake level of R8 exhibited a mild increase according to a cumulative gradient of treatment concentration, but the uptake efficiency of NuBCP-9-R8 conjugate increased dramatically after reaching a 4 μM concentration threshold (Fig. 10). This suggests that a threshold concentration of peptides may be critical for promoting internalization of Rn following conjugation with NuBCP-9, which could

explain the differing performance of NuBCP-9-Rn conjugates at concentrations of 2 μM and 10 μM. The most effective length for intracellular delivery of NuBCP-9 was R10, although unconjugated R12 showed higher uptake efficiency at a concentration of 10 μM (Fig. 11). Many studies have similarly shown that a longer oligoarginines has a higher uptake capacity with a variety of peptide cargo[57,59,60]. With respect to cellular distribution of the internalized peptides, CLSM (Fig. 12) showed results similar to those obtained by flow cytometry (Fig. 11). Unconjugated R8 was distributed into a punctate structure (Fig. 12A), whereas cytosolic labelling was observed in cells treated with NuBCP-9-R8 conjugate at 10 μM (Fig. 12B). It has been reported that R12 shows diffuse cytosolic labelling when its concentration crosses the threshold level[57]. The differing cellular distribution between Rn and NuBCP-9-Rn conjugates administered at concentrations of 10 μM suggests that NuBCP-9 may reduce threshold concentration for effective cytosolic distribution. Overall, NuBCP-9-Rn conjugates may promote cellular uptake at a relatively high concentration.

Many studies have shown that hydrophobic modification increases the uptake efficiency of CPPs[25,26]. Although previous studies considered the N-terminal phenylalanine of NuBCP-9 was important in the enhanced uptake of R8, there is little information about the influence of the C-terminal leucine[31]. In this study, I replaced C-terminal leucine of NuBCP-9-R8 conjugate (FSRSLHSLL-R8) with alanine (FA-R8 conjugate). I found that this Leu-Ala replacement led to a significant decrease in R8 uptake, and that a subsequent replacement of the N-terminal phenylalanine with alanine reduced it further still. My results showed that the N-terminal phenylalanine played a greater role in uptake enhancement than the C-terminal leucine at 10 μM (Fig. 13B). As far as I know, the affinity between Rn and cell membrane decides the cell surface concentration of peptides, which may result in the change of uptake efficiency. The cellular permeability of Rn partly bases on the electrostatic interaction between their guanidinium group with proteoglycan on cell membrane[28]. A enhancement of this interaction may reach because the hydrophobic side chain of amino acids in cargo peptides could immerse into the fatty acid portion of membrane, which reflect the enhancement of affinity[28]. Higher hydrophobic value of phenylalanine from its

aromatic side chain was expected to promote stronger interaction between peptides and membrane than leucine which have an aliphatic side chain[61]. Meanwhile, the aromatic moieties played important role on protein-carbohydrate interactions[62] which may lead more cooperation between NuBCP-9-Rn conjugates entity with proteoglycan on membrane and higher uptake through macropinocytosis. On the other hand, when the treatment concentration was 2 μM, such hydrophobicity replacement had little effect on uptake of R8 (Fig. 13A), which suggests although the enhancement of affinity through hydrophobicity modification may increase the cell surface concentration of peptides, the cell surface concentration may not reach the threshold concentration for effective uptake with relative low treatment concentration. This work suggests that with relative high treatment dose, not only phenylalanine but also leucine in the amino acid sequence of NuBCP-9 makes a contribution to the enhanced uptake of Rn.

For investigating whether the enhanced uptake efficiency of NuBCP-9-Rn conjugates is related to a change in uptake pathway being used, I analyzed the uptake behaviors of Rn and NuBCP-9-Rn conjugates using specific uptake inhibitors. Inhibitors of endocytosis, clathrin-mediated endocytosis[22,23], caveolae-mediated endocytosis[23] and macropinocytosis[21–23], have been proven to partly influence Rn uptake. The uptake behavior of both Rn and NuBCP-9-Rn conjugates were suppressed following treatment with chlorpromazine or EIPA (Fig. 15). In agreement with these findings, Kawaguchi *et al* reported that the uptake of R8 was mediated by both clathrin-mediated endocytosis and macropinocytosis, but not caveolae-mediated endocytosis[22]. Particularly, the inhibition rate with EIPA treatment on uptake of 10 μM peptides was higher than that of 2 μM peptides. Futaki *et al* concluded that macropinocytosis became more prominent when the certain cell surface concentration of Rn was increased[20,53,63]. It suggests that relative high treatment dose lead cell surface accumulation of peptides result in promoted involvement of macropinocytosis on the uptake of Rn and NuBCP-9-Rn conjugates. It is worth noted that F-actin played important role in the macropinocytosis process[21,48]. After using cytochalasin D which is used for inducing depolymerization of F-actin, the reversible cell morphology and reduced internalization of Rn was observed. While, in my results, both clathrin-mediated endocytosis and

macropinocytosis contribute to the internalization of Rn and NuBCP-9-Rn for MDA-MB-231 cells. I discovered that as a commonly used cell line model for studying metastasis, MDA-MB-231 cells have higher F-actin content on membrane for its mobility and migration[64–66]. As a blocker of Na^+/H^+ exchange, EIPA caused reorganization of the F-actin in epithelial cells[67], while CPZ inhibited the effect of phospholipase C [68] which is important to regulate the actin dynamics[69]. So, the other reason for this inhibited effect might depend on the F-actin content of cells, and it needs further study in the future.

In addition to these endocytosis pathways, direct transduction of oligoarginines has also been reported[33,34]. In the presence of chlorpromazine or EIPA, I clearly observed nuclear staining (Fig. 16) in MDA-MB-231 cells treated with Rn or NuBCP-9-Rn conjugates, suggesting nuclear transport of peptides unmediated by endocytosis[23,33].

With low temperature (4 ℃), the internalization pathway preferred to transduction instead of endocytosis, as shown in Fig.18, indicating more cytoplasmic distribution which has also been discovered by other researchers[24]. 4 ℃ treatment showed higher inhibited effect on the uptake of NuBCP-9-Rn conjugates than Rn, especially at 10 μM for NuBCP-9-R8 and NuBCP-9-R10 conjugates (Fig.17), which suggests high participation of endocytosis on uptake of NuBCP-9-Rn conjugates. This might be the other explanation for the enhancement of uptake with NuBCP-9-Rn conjugates. As mentioned before, involvement of macropinocytosis on the uptake of Rn and NuBCP-9-Rn conjugates was promoted at 10 μM (Fig. 15B). Thus, such high participation of endocytosis with NuBCP-9-Rn conjugates treatment might be related with high involvement of macropinocytosis at 10 μM. Besides, promoted macropinocytosis might be related with peptides accumulation on cell membrane caused by higher affinity of NuBCP-9-Rn conjugates. Those observations, in agreement with previous studies, indicate that the uptake of Rn and NuBCP-9-Rn conjugates are partly regulated by clathrin-mediated endocytosis and macropinocytosis, and partly by direct transduction. Besides, NuBCP-9 conjugation on Rn may result in higher participation of endocytosis, especially of macropinocytosis with relative high treatment dose, which may be one possible reason for the enhancement of uptake with NuBCP-9-Rn conjugates.

5. Conclusion

I synthesized peptides in acceptable qualities for evaluating. After analyzing with flow cytometry and CLSM, NuBCP-9 conjugated with Rn enhanced cellular uptake at relative high concentration, which partly involved clathrin-mediate endocytosis and macropinocytosis uptake pathways and partly direct transduction. NuBCP-9-R10 conjugates possessed the highest uptake efficiency at 10 μM. When the treatment dose increased, macropinocytosis became more prominent. Higher participation of endocytosis on uptake of NuBCP-9-Rn conjugates was observed under 4 ℃ treatment. Not only phenylalanine but also leucine in the amino acid sequence of NuBCP-9 makes a contribution to the enhanced uptake of Rn. Therefore, the hydrophobicity of NuBCP-9 might increase the affinity between NuBCP-9-Rn conjugates and cell membrane, promote peptide accumulation on cell surface and activate medication of macropinocytosis, consequently result in the difference of uptake efficiency between NuBCP-9-Rn conjugates and Rn, which needs further study to prove.

Chapter II

Investigation of cytotoxicity of Rn and NuBCP-9-Rn conjugates

1. Introduction

As been proved in chapter I, the uptake of NuBCP-9-Rn conjugates mainly mediated through endocytosis, which suggests the cellular uptake level that measured with flow cytometry including the amount that entrapped in the endosomes. Effective biological based therapy not only depends on the cellular uptake of therapeutic agent via various delivery vectors but also on the ability to escape from endosomes to reach intracellular target for eliciting its effect[16]. Especially for biological macromolecules, it will be faced the acidic and enzymic endosomal environment and endosome membrane barrier[70]. It has been reported that R16 possessed 7 times higher uptake than R8 but they induced similar level of apoptosis when were utilized for delivering pro-apoptotic PAD peptide[21]. Similarly, R8-modified liposomes showed similar internalized capacity with K8-modified liposomes but significant higher gene expression was observed[71]. Those suggest that it is essential to evaluate the biological effect of therapeutic reagent for confirming efficient cytosolic delivery.

B cell lymphoma 2 (BCL-2) family proteins are key regulators of mitochondrial outer membrane permeabilization (MOMP), which is the crucial event to control apoptosis[72–74]. BCL-2 proteins can be divided into anti-apoptotic BCL-2 proteins and pro-apoptotic BCL-2 proteins, all of them share BCL-2 homology (BH) 1- 4 domains[75]. Anti-apoptotic BCL-2 proteins includes Bcl-2 and Bcl-X_L which share all those four BH domains. Pro-apoptotic BCL-2 proteins can be subdivided into effectors and BH3-only proteins. BAX and BAK are typical members of effectors, which share BH 1-3 domains, the oligomerization of effectors is required for inducing MOMP[76,77]. BH3-only proteins, such as tBid, share only α-helical BH3 domains and transduce signals to stimulate oligomerization of effectors[78]. Anti-apoptotic BCL-2 proteins can interact with BH3-only proteins and then sequester its pro-apoptotic effect, which may be one reason for drug-resistance in Bcl-2 overexpression cancer cell lines[79]. Many BH3 peptide–based approaches have been studied for neutralizing the effect of anti-apoptotic BCL-2 proteins, through competitive binding to release the BH3-only proteins and inhibit anti-apoptotic BCL-2 proteins, eventually induce apoptosis of tumor[80–82].

In this research, the therapeutic reagent is NuBCP-9 peptide, which was shown as

a converter of Bcl-2 to promote apoptosis. NuBCP-9 may interact with the loop of Bcl-2 to lead conformation change of Bcl-2 accompany with exposing the BH3 domain of Bcl-2. Release the inhibition of tBid to promote the activation of effectors, in the meantime act as BH3 peptide to bond with Bcl-X_L to inhibit its anti-apoptotic effect[30]. Although NuBCP-9 was firstly proved to act specifically in Bcl-2 overexpression cell lines, Watkins et al. have demonstrated the non-specific cytotoxicity of R8 was magnified by NuBCP-9 conjugation which is unrelated to Bcl-2 expression[31]. Thus, in this chapter, I firstly evaluated the cell viability after treating with NuBCP-9-Rn conjugates. Additionally, for distinguishing the membrane disrupted effect and Bcl-2 related effect, LDH leakage level and apoptosis level were measured in Bcl-2 overexpression cell line, MDA-MB-231. After confirming the efficient cytosolic delivery of NuBCP-9 through the apoptosis results, the suitable length of Rn for intracellular delivery of NuBCP-9 was selected.

2. Materials and Methods

2.1. Materials and Instruments

Name	Source
Rn and NuBCP-9-Rn conjugates peptides	Synthesized and Purified in chapter 1
RPMI-1640	Wako, Japan
Heat-inactivated fetal bovine serum (FBS)	AusGene X, Australia
Penicillin	Wako, Japan
Streptomycin	Wako, Japan
Cell Counting Kit-8	Dojindo Molecular Technologies, Japan
LDH assay kits	Dojindo Molecular Technologies, Japan
Annexin V-FITC apoptosis assay kit	ImmunoChemistry, United States
24-well and 96-well cell culture plate	Violamo, Japan
Falcon 5 ml round-bottom tube, with cell strainer cap	Corning, United States
iMark™ microplate absorbance reader	Bio-Rad Laboratories, United State
BD LSRFortessa X-20 flow cytometer	BD bioscience, United States

2.2. Cell line

The cell lines and culture protocol were same with the description in Chapter I, 2.2.

2.3. Cell viability under Rn and NuBCP-9-Rn conjugates treatment

2.3.1. Influence of co-incubation time on the cell viability

4.5×10^4 /cm^2 MDA-MB-231 cells (in 100 μL culture medium) were seeded into 96-well plates and cultured for 24 h. Change medium with 100 μL of 15 μM NuBCP-9-GX-R8 conjugate contained culture medium and keep incubating for indicated duration at 37 ℃ with 5% CO_2. After incubation, washed cells with 100 μL PBS for 2 times. Cells were continuously incubated in 100 μL peptide-free fresh medium until the total incubation time reaches 24 h at 37 ℃ with 5% CO_2. Then 100 μL Cell Counting Kit-8 (CCK-8) contained culture medium (CCK-8 : medium = 1 : 10 *v*/*v*) was added and keep incubating for 1 h at 37 ℃ with 5% CO_2. Measure the absorbance at 450 nm using microplate absorbance reader.

Cell viability (%) = (T-B) / (C-B) $\times 100$ ----- Equation 1

T: absorbance of treatment group, C: absorbance of control group, B: absorbance of blank (CCK-8 kits contained medium)

2.3.2. Influence of uptake inhibitors on the cell viability

4.5×10^4 /cm^2 MDA-MB-231 cells (in 100 μL culture medium) were seeded into 96-well plates and cultured for 24 h. Change culture medium with 100 μL uptake inhibitors contained culture medium (chlorpromazine, EIPA, and genistein at concentrations of 50, 100, and 200 μM, respectively), pre-incubated cells for 30 min at 37 ℃ with 5% CO_2. Then, the cells were incubated with 15 μM NuBCP-9-R8 conjugate in the absence or presence of inhibitors in 100 μL medium for 2 h at 37 ℃ with 5% CO_2. Or incubated with 100 μL each inhibitor contained medium for 2 h at 37 ℃ with 5% CO_2 as control group, respectively. After incubation, washed cells with 100 μL PBS for 2 times. Cells were continuously incubated in 100 μL inhibitors and peptide-free fresh medium for 22 h at 37 ℃ with 5% CO_2. The following steps were same with the description in 2.3.1.

2.3.3. Evaluating cell viability under Rn and NuBCP-9-Rn conjugates treatment

4.5×10^4 /cm^2 MDA-MB-231 cells (in 100 μL culture medium) were seeded into

96-well plates and cultured for 24 h. Change medium with 100 μL peptide contained culture medium and keep incubating for 2 h at 37 ℃ with 5% CO_2. After incubation, washed cells with 100 μL PBS for 2 times. Cells were continuously incubated in 100 μL peptide-free fresh medium for 22 h at 37 ℃ with 5% CO_2. Then 100 μL CCK-8 contained culture medium (CCK-8 : medium = 1 : 10 *v*/*v*) was added and keep incubating for 1 h at 37 ℃ with 5% CO_2. The following steps were same with the description in 2.3.1.

2.4. Membrane disrupted effect caused by Rn and NuBCP-9-Rn conjugates

4.5×10^4 /cm^2 MDA-MB-231 cells (in 100 μL culture medium) were seeded into 96-well plates and cultured for 24 h. Media change was given with 100 μL medium containing 10 μM peptides, and the cells were incubated for 2 h at 37 ℃ with 5% CO_2. For making high control, 10 μL lysis buffer was added into wells which were incubated with peptide-free medium and incubated for 30min at 37 ℃ with 5% CO_2. After incubation, added 100 μL Working Solution into each well, and incubate the plate at 37 ℃ for 15min protected from light. Then 50 μL Stop Solution was added. Measure the absorbance of plate at 450 nm using microplate absorbance reader.

LDH leakage level (%) = (T-C) / (H-C) ×100 ----- Equation 2

T: absorbance of treatment group, C: absorbance of low control group, H: absorbance of high control group

2.5. Apoptosis level induced by NuBCP-9-Rn conjugates

2.5.1. Determination of the treatment condition for making positive control group

4.5×10^4 /cm^2 MDA-MB-231 cells (in 100 μL culture medium) were seeded into 96-well plates and cultured for 24 h. Change medium with 100 μL camptothecin contained culture medium and keep incubating for 4 h at 37 ℃ with 5% CO_2. The following steps were same with the description in 2.3.2.

2.5.2. Apoptosis level induced by peptides

4.5×10^4 /cm^2 MDA-MB-231 cells (in 0.5 mL culture medium) were seeded into

24-well plates and cultured for 24 h. Then, the cells were incubated in 0.4 mL culture medium containing 10 μM peptides for 2 h at 37 ℃ with 5% CO_2. The cells were washed with 0.5 mL PBS and continuously incubated in 0.5 mL peptide-free culture medium for 22 h at 37℃ with 5% CO_2. In the positive control group, cells were incubated in 0.4 mL culture medium containing 5 μM camptothecin for 4 h at 37℃ with 5% CO_2. After trypsinization, the cells were collected and centrifuged at 300 g for 3 min. Following a PBS wash, cells were suspended in 100 μL ice-cold 1× binding buffer (10× binding buffer : diH_2O = 1 : 9 *v*/*v*). Then, the cells were labeled with 5 μL fresh Annexin-V-FITC staining solution (200× Annexin V-FITC reagent : PBS = 1 : 9 *v*/*v*) and 5 μL fresh propidium iodide (PI) staining solution (250 μg/ml PI reagent : PBS = 1 : 1 *v*/*v*) on ice for 10 minutes in the dark. 10,000 cell pellets were analyzed immediately by BD LSRFortessa X-20 flow cytometer. The blue 488-nm laser was used for excitation of FITC and PI, and their fluorescence intensity was detected by a 525/30 BP filter and 575/26 BP filter, respectively.

2.6. Statistical Analysis

All comparisons of mean values were performed using analysis of variance test (ANOVA). Multiple comparisons among all groups were performed using two-way ANOVA with Bonferroni test. For comparisons between control and treatment groups, Dunnett test was used. Results yielding a *p* value less than 0.05 were considered statistically significant.

3. Results

3.1. Cell viability under Rn and NuBCP-9-Rn conjugates treatment

The WST-8 assay is one of the most popular tests to assess the toxicity of potential compounds[83]. Tetrazolium salt reduction to formazan occurs in the mitochondria of living cells due to the activity of mitochondrial dehydrogenases (in particular, succinate dehydrogenase)[84,85]. The amount of the formazan dye, generated by the activities of dehydrogenases in cells, is directly proportional to the number of living cells. In this

part, WST-8 assay was used for evaluating the cell viability due to its convenience and sensitivity.

3.1.1. Influence of co-incubation time on the cell viability

Firstly, the cell viability of MDA-MB-231 cells that were treated with 15 μM NuBCP-9-GX-R8 conjugate was determined after different co-incubation time. As can be seen in Fig. 19, with the extension of co-incubation duration, the cell viability was decreased, but there was no significant difference between 2 h and 4 h co-incubation group. Considering with the cellular uptake results in chapter I (Fig.9), 2 h co-incubation duration might be sufficient for intracellular delivery of peptide. Thus, 2 h was chose as the co-incubation duration for the following studies.

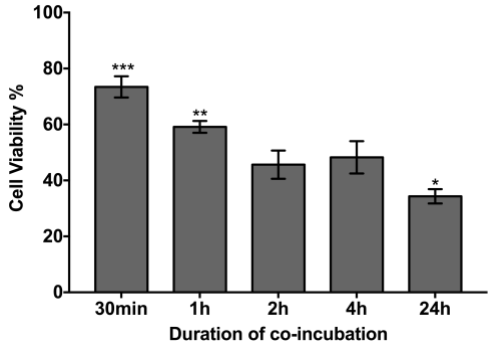

Fig.19 Influence of co-incubation time on the cell viability of MDA-MB-231 cells.
Viability of MDA-MB-231 cells following 30 min, 1, 2, 4, 24 h co-incubation with 15 μM NuBCP-9-GX-R8 conjugate contained medium and continuous incubating in peptide-free medium at 37 ℃ with 5% CO_2 until the total incubation time reaching 24 h. Each value represents the mean ± SD from triplicate experiments.
(ANOVA, Bonferroni test, compare with 2 h-treatment group, $^{*}p < 0.05$, $^{**}p < 0.01$, $^{***}p < 0.001$)

3.1.2. Influence of uptake inhibitors on the cell viability

As been proved in chapter I, the uptake of NuBCP-9-Rn was inhibited by CPZ and EIPA (Fig.15). Thus, it is valuable to investigate if such uptake suppression has effect on the cytotoxicity of MDA-MB-231 cells that caused by NuBCP-9-R8 conjugate. After treating MDA-MB-231 cells with 15 μM NuBCP-9-R8 conjugate in absence or presence of three uptake inhibitors, 50 μM CPZ or 100 μM EIPA significantly reduced the cytotoxicity that caused by NuBCP-9-R8 conjugate, while there is little effect of 200 μM genistein on the toxic-effect of NuBCP-9-R8 conjugate (Fig.20).

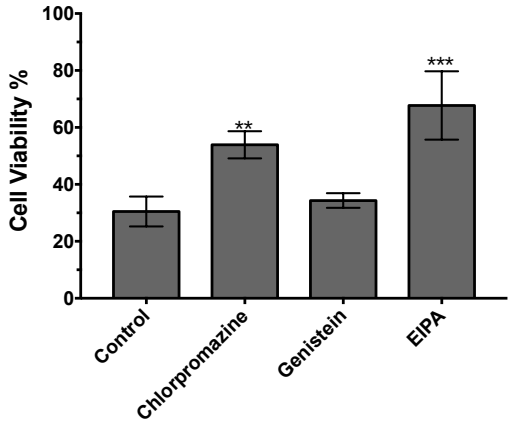

Fig.20 Influence of uptake inhibitors on the cell viability of MDA-MB-231 cells.
Viability of MDA-MB-231 cells following 2 h treatment with 15 μM NuBCP-9-R8 conjugate in the absence or presence of 50 μM CPZ, 200 μM genistein or 100 μM EIPA, respectively and continuous incubating in inhibitors and peptide-free medium for 22 h at 37 ℃ with 5% CO_2. Each value represents the mean ± SD from triplicate experiments.
(ANOVA, Dunnett test, compare with control group, $^{**}p < 0.01$, $^{***}p < 0.001$)

3.1.3. Evaluating cell viability under Rn and NuBCP-9-Rn conjugates treatment

The cell viability was measured in Bcl-2 overexpress cell line MDA-MB-231. In this research, I used the linker sequence GGG for conjugating NuBCP-9 with oligoarginines, it showed that no significant difference of cytotoxicity of NuBCP-9-R8 comparing with peptide using the linker GAhx (GX) which was used in published articles[30] (Fig.21A). Up to 15 μM, negative control peptide FA - R8 and AA - R8 were relatively non-toxic, while NuBCP-9-R8 conjugate induced 56.85% ± 6.18% cell death (Fig.21B). The results (Fig.21C) showed that the cells treated with NuBCP-9, NuBCP-9-R4 or NuBCP-9-R6 conjugates were viable up to 15 μM. When the arginine residuals of Rn were more than eight, NuBCP-9-Rn (n = 8, 10, 12, and 14) showed concentration dependent cytotoxicity. NuBCP-9 with longer Rn had lower IC_{50} (Tab.5). When the cells treated with Rn, there was little cytotoxicity with R8, R10 and R12 up to 15 μM. R14 showed low toxicity under 10 μM, but only 46.08% ± 6.58% cells were survival at 15 μM (Fig.21D).

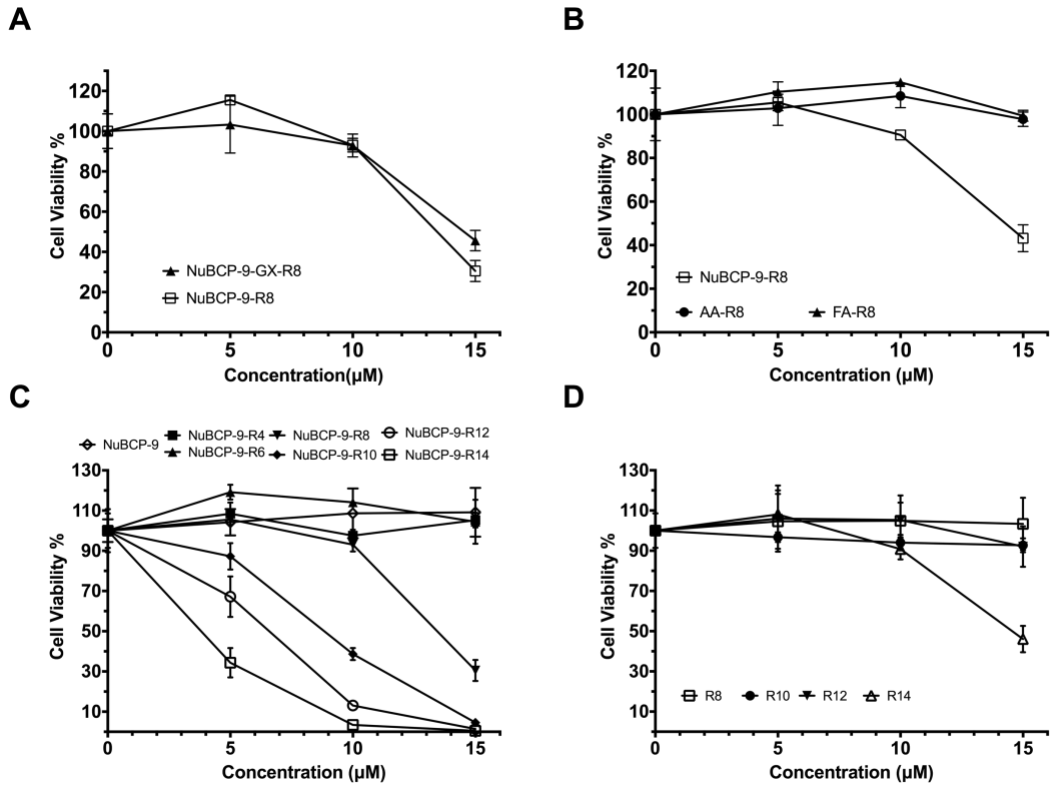

Fig. 21 Cell viability of MDA-MB-231 cells under Rn and NuBCP-9-Rn conjugates treatment. Viability of MDA-MB-231 cells following a 2 h incubation with 0 - 15 μM indicated unlabeled peptides and then a 22 h incubation in the absence of peptides at 37 ℃ with 5% CO_2. Each value represents the mean ± SD from triplicate experiments. Unlabeled peptides refer to (A) NuBCP-9-R8 and NuBCP-9-GX-R8 conjugates (B) NuBCP-9-R8, AA-R8 and FA-R8 conjugates (C) NuBCP-9-Rn (n = 0, 4, 6, 8, 10, 12, and 14) conjugates (D) Rn (n = 8, 10, 12 and 14), respectively.

Tab. 5 IC50 of Rn and NuBCP-9-Rn conjugates (n = 8, 10, 12 and 14) in MDA-MB-231 cells.

Number of arginine (n)	IC_{50} (μM)	
	Rn	NuBCP-9-Rn
8	N.D.	13.51
10	N.D.	8.31
12	N.D.	6.08
14	14.58	4.10

(Abbreviation: N.D., not done)

3.2. Membrane disrupted effect caused by Rn and NuBCP-9-Rn conjugates

The cytotoxicity of NuBCP-9-Rn conjugates did not correlate well with their uptake efficiency as determined by flow cytometry. Rn induces non-specific cytotoxicity at high doses owing to its strong electrostatic interaction with the cell membrane[19,21]. Furthermore, a non-specific necrotic effect induced by NuBCP-9-R8

conjugate has also been demonstrated in previous studies. Therefore, I considered the possibility that membrane integrity may be disturbed by short-time incubation of cells with the peptides.

When the cell membranes are compromised or damaged, lactate dehydrogenase (LDH) is released into the surrounding extracellular space. Since this only happens when cell membrane integrity is compromised, the present of this enzyme in the culture medium can be used as a biomarker for cytolysis[86]. It has been widely used to evaluate the destruction of membrane integrity by positive charged components such as cationic liposomes[87], cationic polymers[88], and penetrating peptides[89]. Thus, in this part I measured cellular LDH leakage levels after treatment with peptides to estimate membrane disruption.

As can be seen in Fig. 22, following conjugation with NuBCP-9, LDH release increased with increasing length of Rn. NuBCP-9-R12 and NuBCP-9-R14 conjugates induced 43.97% ± 0.65% and 76.09% ± 1.59% (n = 3) LDH release at 10 μM, respectively. While unconjugated Rn (n = 8, 10, and 12) caused negligible membrane disruption in MDA-MB-231 cells at 10 μM, the most toxic peptide, R14, disturbed membrane integrity of 5.94% ± 0.32% cells, which is still significantly less membrane damage than that caused by the conjugates.

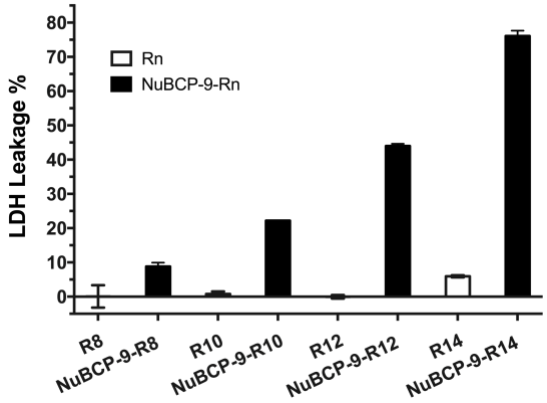

Fig. 22 LDH leakage level induced by Rn and NuBCP-9-Rn conjugates.
LDH leakage level in MDA-MB-231 cells following a 2 h incubation with 10 μM unlabeled Rn and NuBCP-9-Rn (n = 8, 10, 12 and 14) conjugates at 37 ℃ with 5% CO_2. Each value represents the mean ± SD from triplicate experiments.

3.3. Apoptosis level induced by NuBCP-9-Rn conjugates

For apoptosis and necrosis measurement, Annexin V-FITC/PI method is commonly used[90]. In early-apoptotic cells, phosphotidylserine (PS) flips from the inside of the cell membrane to the surface of the cell membrane. Annexin-V, a Ca^{2+}-dependent phospholipid binding protein, could conjugate to PS sites on the membrane surface with high affinity. Propidium iodide (PI) labeled the cellular DNA in necrotic cells where the cell membrane has been totally compromised[91]. This combination could distinguish the cell state among early apoptotic cells (Annexin-V positive, PI negative), necrotic cells (Annexin-V positive, PI positive), and viable cells (Annexin-V negative, PI negative)[92]. Thus, Annexin-V FITC/PI staining was used for analyzing the apoptosis level that induced by NuBCP-9-Rn conjugates in this part.

3.3.1. Determination of the treatment condition for making positive control group

Before determining the apoptosis level induced by NuBCP-9-Rn conjugates, the suitable condition for making positive control should be determined. It is recommended that apoptosis may be induced with 2 - 4 μg/mL (5.7 μM - 11.5 μM) camptothecin over 4 h treatment following kits protocol, while the results may be various with each cell line. Camptothecin has been proved to induce apoptosis in various cell lines[93,94]. Thus, I measured the cell viability of MDA-MB-231 following 4 h treatment with 0 – 10 μM camptothecin. From the results in Fig. 23, all the treatment with camptothecin showed significant cytotoxicity. When treatment dose was over 4 μM, the degree of cytotoxicity change was decreased. Considering with the published articles[95,96], 4 h treatment with 5 μM camptothecin was decided as condition for making positive control group.

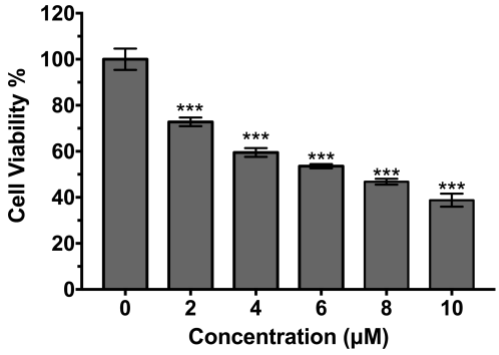

Fig. 23 Cell viability of MDA-MB-231 cells under camptothecin treatment.
Viability of MDA-MB-231 cells following a 4 h incubation with 0 - 10 μM camptothecin at 37 ℃ with 5% CO_2. Each value represents the mean ± SD from triplicate experiments.
(ANOVA, Dunnett test, compare with non-treatment group, $^{***}p < 0.001$)

3.3.2. Apoptosis level induced by peptides

The mechanism of cell death caused by NuBCP-9 has been reported as pro-apoptosis, occurring through exposing BH3 domain of Bcl-2[30]. In our study, we detected the level of apoptosis induced by 10 μM of NuBCP-9-R8 conjugate, NuBCP-9-R10 conjugate, and R10. Following staining with annexin V-FITC and propidium iodide (PI), MDA- MB-231 cells were analyzed by flow cytometry. From Fig. 24, it can be seen that R10- treated cells and the negative control group showed similar levels of apoptosis. NuBCP-9-R10 conjugate induced more apoptosis and necrosis than NuBCP-9-R8 conjugate at 10 μM.

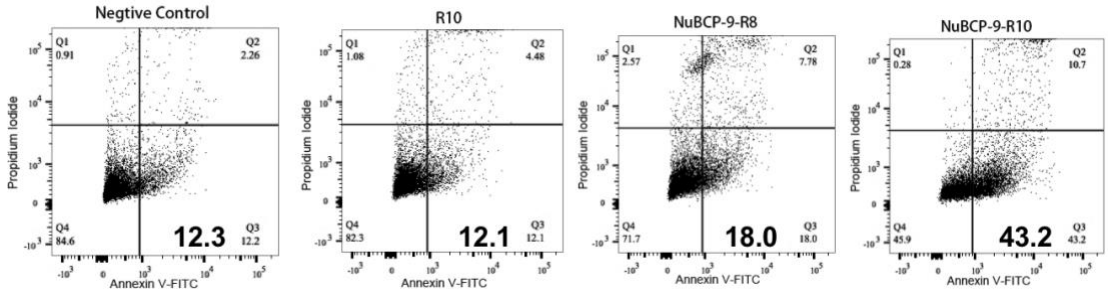

Fig. 24 Apoptosis levels induced by peptides in MDA-MB-231 cells.
After a 2 h incubation with 10 μM unlabeled NuBCP-9-R8, NuBCP-9-R10 conjugates and R10 and then a 22 h incubation in their absence, apoptosis was induced in MDA- MB-231 cells. 4 h treatment with 5 μM camptothecin at 37 ℃ with 5% CO_2 was proceeded as positive control group. The level of apoptosis was determined from Annexin-V/PI staining observed by flow cytometry. 10,000 counts were taken for each sample.

4. Discussion

Effective uptake and endosomal escape are important to ensure cellular efficacy of the therapeutic entity. The aim of research in this part is to study cellular cytotoxicity caused by NuBCP-9 conjugation Rn of different lengths for confirming the efficient cytosolic delivery of peptides.

Firstly, WST-8 assay was used for evaluating cell viability after peptides treatments. Through the cell viability results with different co-incubation duration (Fig. 19), 2 h may be sufficient for intracellular delivery of NuBCP-9-Rn conjugates. Tunnemann *et al* showed that the peptides comprising the proliferating cell nuclear antigen binding domain was fused with CPPs (TAT), even 10 min co-incubation duration with following

6h peptide-absent incubation was sufficient to inhibit proliferation of about 30% mouse myoblasts[97]. Thus, 2 h co-incubation duration was selected as the conditions for following studies.

In chapter I, the uptake of NuBCP-9-Rn conjugates was partly mediated by clathrin-mediated endocytosis and macropinocytosis. The treatment with uptake inhibitors CPZ or EIPA partly decreased the cytotoxicity by 15 μM of NuBCP-9-R8 conjugate, but not with genistein (Fig.20). It suggests the cytotoxicity by NuBCP-9-R8 conjugate partly due to its Bcl-2 targeted proapoptotic effect, which related with the uptake level.

Up to a concentration of 15 μM, NuBCP-9, NuBCP-9-R4 and NuBCP-9-R6 conjugates induced slight toxicity, while NuBCP-9 with longer Rn (n = 8, 10, 12, and 14) resulted in greater cytotoxicity at the same dose (Fig. 21C). Without conjugation, only R14 led to severe cellular toxicity at 15 μM (Fig. 21D), suggesting that NuBCP-9 is the source of the differing cytotoxicity between conjugated and unconjugated Rn. NuBCP-9-R14 conjugate showed the highest cytotoxicity in MDA-MB-231 cells. However, NuBCP-9-R10 conjugate exhibited the most effective uptake as determined by flow cytometry in chapter I (Fig.11B). This limited correlation between uptake level and cytotoxicity suggests that the Bcl-2-based mechanism of internalized peptides was not the only source of NuBCP-9-Rn conjugates-induced cytotoxicity.

The non-specific cytotoxicity from relatively long Rn was caused by membrane disruption resulting from the high density positive charge formed around the cell membrane. This can also be seen in studies where R16 exhibits higher non-specific cytotoxicity and uptake efficiency than R8[19,21,58]. Furthermore, a non-specific necrotic effect induced by NuBCP-9-R8 conjugate has also been demonstrated in previous studies[31]. Thus, it is assumed that the poor correlation between uptake level and cytotoxicity is the result of necrosis unrelated to Bcl-2. Therefore, to evaluate non-specific cytotoxicity, I chose to determine the level of membrane disruption caused by Rn and NuBCP-9-Rn conjugates. NuBCP-9 conjugated with R12 and R14 induced more LDH release at a concentration of 10 μM and were therefore deemed to cause intolerable non-specific cytotoxicity. However, without NuBCP-9 conjugation, even

R14 had only negligible effects on membrane integrity, as shown in Fig. 22. These results suggest NuBCP-9 aggravates the membrane perturbance caused by R12 and R14. For this reason, R12 and R14 may not be suitable choices for conjugation with NuBCP-9 in this context.

On a related point, the decreasing uptake levels of NuBCP-9-R12 and NuBCP-9-R14 conjugates at concentrations of 10 μM in MDA-MB-231 cells when compared to that of the NuBCP-9-R10 conjugate in chapter I (Fig. 11B) might be explained by non-specific cytotoxicity resulting in poor membrane integrity, which in turn makes it impossible for the internalized peptides to remain within the cells long enough to exert their full effects.

Finally, NuBCP-9 has been proven to act through Bcl-2 to induce apoptosis[30]. After evaluating the LDH leakage level, I detected the level of apoptosis induced by NuBCP-R8 and NuBCP-9-R10 conjugates. Just as in chapter I-Fig. 11B, Fig. 24 shows that NuBCP-9-R10 conjugate induced a higher level of apoptosis than NuBCP-9-R8 conjugate, which might reflect the correlation between uptake capacity and intracellular activity. Nakase et al. showed that the level of apoptosis induced by pro-apoptotic domain peptide (PAD)-Rn conjugates was related to intracellular uptake level[21]. Taking this into consideration, the higher level of apoptosis induced by NuBCP-9-R10 conjugate may be related to its relatively high cellular uptake and efficient cytosolic delivery, which can lead to more specific interaction between NuBCP-9 and Bcl-2 in MDA-MB-231 cells.

5. Conclusion

NuBCP-9-Rn conjugates showed Rn length-dependent cytotoxicity in MDA-MB-231 cells, which limited correlation with uptake level shown in chapter I. It suggests that the Bcl-2-based mechanism of internalized peptides was not the only source of NuBCP-9-Rn conjugates-induced cytotoxicity. The reason for this limited correlation is that NuBCP-9 conjugation significantly enhanced the membrane disrupted effect of Rn. In this case, R12 and R14 led intolerable membrane disruption after conjugating with NuBCP-9, which suggests they are not suitable for the therapeutic use of NuBCP-

9. NuBCP-9-R10 conjugate induced highest level of apoptosis, which reflected the efficient cytosolic delivered level of peptides. Overall, NuBCP-9-R10 conjugate is the most suitable compound for pro-apoptotic therapeutic application of NuBCP-9.

Conclusion

In this study, I have synthesized the Rn and NuBCP-9-Rn conjugates for following studies. The cellular uptake and distribution of Rn have been compared before or after conjugating with NuBCP-9. Through hydrophobic replacement and analyzing uptake pathways, the uptake mechanism of NuBCP-9-Rn conjugates has been discussed. The membrane disrupted effect and apoptosis level have been studied for resolving the cytotoxicity of NuBCP-9-Rn conjugates.

1. Cellular uptake and distribution of Rn and NuBCP-9-Rn conjugates

In MDA-MB-231 cells, the uptake of NuBCP-9-R8 conjugate was found to be significantly higher than that of R8 when the peptide dose was above 4 μM. NuBCP-9-Rn (n= 6, 8, 10, 12 and 14) conjugates showed significantly increased uptake than Rn with same numbers of arginine at 10 μM but not at 2 μM. R12 was the most effective length for cellular delivery of NuBCP-9 at 2 μM, while it altered to be R10 at 10 μM. Under CLSM, 2 μM Rn and NuBCP-9-Rn conjugates labelled punctate vesicles. Besides, at 10 μM, NuBCP-9 conjugation promoted the cytoplasmic diffusion of peptides. The NuBCP-9-R10 conjugate exhibited the strongest cellular fluorescence signal. Those are in agreement with the flow cytometry results. Overall, at relative high dose, NuBCP-9 conjugation promoted the uptake of Rn. While the enhanced degree was various with different Rn. NuBCP-9-R10 conjugate possessed highest uptake efficiency at 10 μM in MDA-MB-231 cells.

2. Uptake mechanism of Rn and NuBCP-9-Rn conjugates

Distal hydrophobic amino acids replacement played a role in uptake enhancement of NuBCP-9-R8 conjugate than R8 at 10 μM. The uptake of Rn and NuBCP-9-Rn conjugates was mediated by clathrin-mediated endocytosis and macropinocytosis. When treatment dose of peptides was increased from 2 to 10 μM, the involvement of macropinocytosis was increased. Treatment of 4 ℃ significantly suppressed the uptake

of peptides, especially for NuBCP-9-Rn conjugates. Cytoplasmic diffusion and nucleus staining were observed when the uptake of peptides was partly inhibited by 4℃ treatment or uptake inhibitors, which suggests the participation of direct transduction in the uptake of Rn and NuBCP-9-Rn conjugates. The hydrophobicity of NuBCP-9 might increase the affinity between NuBCP-9-Rn conjugates and cell membrane, promote peptide accumulation on cell surface and activate medication of macropinocytosis, consequently result in the difference of uptake efficiency between NuBCP-9-Rn conjugates and Rn.

3. Cytotoxicity of Rn and NuBCP-9-Rn conjugates

As the length of Rn increased, the cytotoxicity of NuBCP-9-Rn conjugates were increased in MDA-MB-231 cells, which had limited correlation with uptake level. It suggests that the Bcl-2-based mechanism of internalized peptides was not the only source of NuBCP-9-Rn conjugates-induced cytotoxicity. Following conjugation with NuBCP-9, LDH release increased with increasing length of Rn. NuBCP-9-R12 and NuBCP-9-R14 conjugates induced severe membrane damage at 10 μM. It suggests that R12 and R14 may not be suitable choices for conjugation with NuBCP-9. NuBCP-9-R10 conjugate induced more apoptosis than NuBCP-9-R8 conjugate at 10 μM. It suggests the higher level of apoptosis induced by NuBCP-9-R10 conjugate may be related to its relatively high cellular uptake level, which reflected its cytosolic delivery level.

In this study, the influence of NuBCP-9 conjugation on cellular uptake and cytotoxicity have been discussed. NuBCP-9-R10 conjugate has been selected as the most suitable compound for pro-apoptotic therapeutic application of NuBCP-9. The information in this study will be valuable in the design of therapeutic peptide conjugated with oligoarginines for anti-cancer therapy.

Acknowledgements

Above all, great acknowledge is made to all those who helped me on my life and study during the past three years of my stay in Nagasaki University.

My deepest gratitude goes first and foremost to my supervisor, Prof. Shigeru Kawakami, for his acceptance of me as a Ph.D. candidate three years ago and support to my life and study progress during the past three years.

Second, I would like to express my heartfelt gratitude to associate professor Masayori Hagimori, who put great effort on solving the technical issues related my researches, which provided the concrete support for my study.

I am also deeply indebted to assistant professor Yuki Fuchigami, although she has already transferred as a visiting researcher. She put considerable time on solving the problems related my researches and provided great concern of my life.

Besides, special thanks should go to Prof. Naotaka Kuroda, who made it possible for my further study in Nagasaki University as a Ph.D. candidate.

Finally, I feel grateful to all my lab colleagues including those who have already graduated, especially Mr. Tadaharu Suga. I am so thankful for his support through my entire research. All of you gave me considerable support and understanding on my living and study here. And I greatly appreciate my families' support and endless love.

Publication

Wei Wang, Tadaharu Suga, Masayori Hagimori, Naotaka Kuroda, Yuki Fuchigami, and Shigeru Kawakami, Investigation of intracellular delivery of the NuBCP-9 by conjugation with oligoarginines peptides in MDA-MB-231 cells. *Biol. Pharm. Bull.*, **41**, 1448–1455 (2018)

Reference

1. Ellerby, HM, Arap, W, Ellerby, LM, Kain, R, Andrusiak, R, Del Rio, G, *et al.* (1999). Anti-cancer activity of targeted pro-apoptotic peptides. *Nat. Med.* **5**: 1032.
2. Raina, D, Kosugi, M, Ahmad, R, Panchamoorthy, G, Rajabi, H, Alam, M, *et al.* (2011). Dependence on the MUC1-C oncoprotein in non–small cell lung cancer cells. *Mol. Cancer Ther.* **10**: 806–816.
3. Orzechowska, EJ, Kozlowska, E, Czubaty, A, Kozlowski, P, Staron, K and Trzcinska-Danielewicz, J (2014). Controlled delivery of BID protein fused with TAT peptide sensitizes cancer cells to apoptosis. *BMC Cancer* **14**: 771.
4. Kim, D, Lee, I-H, Kim, S, Choi, M, Kim, H, Ahn, S, *et al.* (2014). A specific STAT3-binding peptide exerts antiproliferative effects and antitumor activity by inhibiting STAT3 phosphorylation and signaling. *Cancer Res.* **74**: 2144–2151.
5. Alves, ID, Carré, M, Montero, M-P, Castano, S, Lecomte, S, Marquant, R, *et al.* (2014). A proapoptotic peptide conjugated to penetratin selectively inhibits tumor cell growth. *Biochim. Biophys. Acta (BBA)-Biomembranes* **1838**: 2087–2098.
6. Ko, YT, Falcao, C and Torchilin, VP (2009). Cationic liposomes loaded with proapoptotic peptide D-(KLAKLAK) 2 and Bcl-2 antisense oligodeoxynucleotide G3139 for enhanced anticancer therapy. *Mol. Pharm.* **6**: 971–977.
7. Duvall, CL, Convertine, AJ, Benoit, DSW, Hoffman, AS and Stayton, PS (2010). Intracellular delivery of a proapoptotic peptide via conjugation to a RAFT synthesized endosomolytic polymer. *Mol. Pharm.* **7**: 468–476.
8. Standley, SM, Toft, DJ, Cheng, H, Soukasene, S, Chen, J, Raja, SM, *et al.* (2010). Induction of cancer cell death by self-assembling nanostructures incorporating a cytotoxic peptide. *Cancer Res.* **70**: 3020–3026.
9. Hasegawa, M, Sinha, RK, Kumar, M, Alam, M, Yin, L, Raina, D, *et al.* (2015). Intracellular Targeting of the Oncogenic MUC1-C Protein with a Novel GO-203 Nanoparticle Formulation **2**: 2338–2348.
10. Kinoshita, M and Hynynen, K (2005). Intracellular delivery of Bak BH3 peptide by microbubble-enhanced ultrasound. *Pharm. Res.* **22**: 716–720.
11. Kapoor, S, Gupta, D, Kumar, M, Sharma, S, Gupta, AK, Misro, MM, *et al.* (2016). Intracellular delivery of peptide cargos using polyhydroxybutyrate based biodegradable nanoparticles: Studies on antitumor efficacy of BCL-2 converting peptide, NuBCP-9. *Int. J. Pharm.* **511**: 876–889.
12. Kumar, M, Gupta, D, Singh, G, Sharma, S, Bhat, M, Prashant, CK, *et al.* (2014). Novel polymeric nanoparticles for intracellular delivery of peptide cargos: antitumor efficacy of the BCL-2 conversion peptide NuBCP-9. *Cancer Res.* **74**: 3271–3281.
13. Heitz, F, Morris, MC and Divita, G (2009). Twenty years of cell-penetrating peptides: from molecular mechanisms to therapeutics. *Br. J. Pharmacol.* **157**: 195–206.
14. Raucher, D and Ryu, JS (2015). Cell-penetrating peptides : strategies for anticancer treatment. *Trends Mol. Med.* **21**: 560–570.
15. Frankel, AD and Pabo, CO (1988). Cellular uptake of the tat protein from human immunodeficiency virus. *Cell* **55**: 1189–1193.

16. El-Sayed, A, Futaki, S and Harashima, H (2009). Delivery of macromolecules using arginine-rich cell-penetrating peptides: ways to overcome endosomal entrapment. *AAPS J.* **11**: 13–22.
17. Dokka, S, Toledo-Velasquez, D, Shi, X, Wang, L and Rojanasakul, Y (1997). Cellular delivery of oligonucleotides by synthetic import peptide carrier. *Pharm. Res.* **14**: 1759–1764.
18. Fernández-Carneado, J, Kogan, MJ, Pujals, S and Giralt, E (2004). Amphipathic peptides and drug delivery. *Pept. Sci.* **76**: 196–203.
19. Mitchell, DJ, Steinman, L, Kim, DT, Fathman, CG and Rothbard, JB (2000). Polyarginine enters cells more efficiently than other polycationic homopolymers. *Chem. Biol. Drug Des.* **56**: 318–325.
20. Futaki, S, Hirose, H and Nakase, I (2013). Arginine-rich Peptides : Methods of Translocation Through Biological Membranes *Curr. Pharm. Des.* **19**: 2863–2868.
21. Nakase, I, Niwa, M, Takeuchi, T, Sonomura, K, Kawabata, N, Koike, Y, *et al.* (2004). Cellular Uptake of Arginine-Rich Peptides : Roles for Macropinocytosis and Actin Rearrangement. *Mol. Ther.* **10**: 1011–1022.
22. Kawaguchi, Y, Takeuchi, T, Kuwata, K, Chiba, J, Hatanaka, Y, Nakase, I, *et al.* (2016). Syndecan-4 is a receptor for clathrin-mediated endocytosis of arginine-rich cell-penetrating peptides. *Bioconjug. Chem.* **27**: 1119–1130.
23. Duchardt, F, Fotin-Mleczek, M, Schwarz, H, Fischer, R and Brock, R (2007). A comprehensive model for the cellular uptake of cationic cell-penetrating peptides. *Traffic* **8**: 848–866.
24. Zaro, JL and Shen, W-C (2005). Evidence that membrane transduction of oligoarginine does not require vesicle formation. *Exp. Cell Res.* **307**: 164–173.
25. Sayers, EJ, Cleal, K, Eissa, NG, Watson, P and Jones, AT (2014). Distal phenylalanine modification for enhancing cellular delivery of fluorophores, proteins and quantum dots by cell penetrating peptides. *J. Control. Release* **195**: 55–62.
26. Takayama, K, Nakase, I, Michiue, H, Takeuchi, T, Tomizawa, K, Matsui, H, *et al.* (2009). Enhanced intracellular delivery using arginine-rich peptides by the addition of penetration accelerating sequences (Pas). *J. Control. Release* **138**: 128–133.
27. Pham, W, Kircher, MF, Weissleder, R and Tung, C (2004). Enhancing membrane permeability by fatty acylation of oligoarginine peptides. *Chembiochem* **5**: 1148–1151.
28. Shental-Bechor, D, Haliloglu, T and Ben-Tal, N (2007). Interactions of cationic-hydrophobic peptides with lipid bilayers: a Monte Carlo simulation method. *Biophys. J.* **93**: 1858–1871.
29. Hirose, H, Takeuchi, T, Osakada, H, Pujals, S, Katayama, S, Nakase, I, *et al.* (2012). Transient focal membrane deformation induced by arginine-rich peptides leads to their direct penetration into cells. *Mol. Ther.* **20**: 984–993.
30. Kolluri, SK, Zhu, X, Zhou, X, Lin, B, Chen, Y, Sun, K, *et al.* (2008). A short Nur77-derived peptide converts Bcl-2 from a protector to a killer. *Cancer Cell* **14**: 285–298.
31. Watkins, CL, Sayers, EJ, Allender, C, Barrow, D, Fegan, C, Brennan, P, *et al.* (2011). Co-operative membrane disruption between cell-penetrating peptide and cargo: implications for the therapeutic use of the Bcl-2 converter peptide D-NuBCP-9-r8. *Mol. Ther.* **19**: 2124–2132.
32. Arisan, ED, Kutuk, O, Tezil, T, Bodur, C, Telci, D and Basaga, H (2010). Small inhibitor of Bcl-2, HA14-1, selectively enhanced the apoptotic effect of cisplatin by modulating Bcl-2 family members in MDA-MB-231 breast cancer cells. *Breast Cancer Res. Treat.* **119**: 271.
33. Haldar, S, Negrini, M, Monne, M, Sabbioni, S and Croce, CM (1994). Down-regulation of bcl-

2 by p53 in breast cancer cells. *Cancer Res.* **54**: 2095–2097.

34. Zapata, JM, Krajewska, M, Krajewski, S, Huang, R-P, Takayama, S, Wang, H-G, *et al.* (1998). Expression of multiple apoptosis-regulatory genes in human breast cancer cell lines and primary tumors. *Breast Cancer Res. Treat.* **47**: 129–140.
35. Merrifield, RB (1963). Solid phase peptide synthesis. I. The synthesis of a tetrapeptide. *J. Am. Chem. Soc.* **85**: 2149–2154.
36. Suga, T, Fuchigami, Y, Hagimori, M and Kawakami, S (2017). Ligand peptide-grafted PEGylated liposomes using HER2 targeted peptide-lipid derivatives for targeted delivery in breast cancer cells: The effect of serine-glycine repeated peptides as a spacer. *Int. J. Pharm.* **521**: 361–364.
37. Aguilar, M-I (2004). HPLC of Peptides and Proteins. *HPLC Pept. Proteins*, Springer: pp 3–8.
38. Hazama, H, Nagao, H, Suzuki, R, Toyoda, M, Masuda, K, Naito, Y, *et al.* (2008). Comparison of mass spectra of peptides in different matrices using matrix-assisted laser desorption/ionization and a multi-turn time-of-flight mass spectrometer, MULTUM-IMG. *Rapid Commun. Mass Spectrom.* **22**: 1461–1466.
39. Fretz, MM, Penning, NA, Al-Taei, S, Futaki, S, Takeuchi, T, Nakase, I, *et al.* (2007). Temperature-, concentration-and cholesterol-dependent translocation of L-and D-octa-arginine across the plasma and nuclear membrane of CD34+ leukaemia cells. *Biochem. J.* **403**: 335–342.
40. Futaki, S, Suzuki, T, Ohashi, W, Yagami, T, Tanaka, S, Ueda, K, *et al.* (2001). Arginine-rich peptides An abundant source of membrane-permeable peptides having potential as carriers for intracellular protein delivery. *J. Biol. Chem.* **276**: 5836–5840.
41. Brewer, CF and Riehm, JP (1967). Evidence for possible nonspecific reactions between N-ethylmaleimide and proteins. *Anal. Biochem.* **18**: 248–255.
42. Prudent, M and Girault, HH (2009). The role of copper in cysteine oxidation: study of intra-and inter-molecular reactions in mass spectrometry. *Metallomics* **1**: 157–165.
43. Hansen, RE and Winther, JR (2009). An introduction to methods for analyzing thiols and disulfides: Reactions, reagents, and practical considerations. *Anal. Biochem.* **394**: 147–158.
44. Getz, EB, Xiao, M, Chakrabarty, T, Cooke, R and Selvin, PR (1999). A comparison between the sulfhydryl reductants tris (2-carboxyethyl) phosphine and dithiothreitol for use in protein biochemistry. *Anal. Biochem.* **273**: 73–80.
45. Henkel, M, Röckendorf, N and Frey, A (2016). Selective and efficient cysteine conjugation by maleimides in the presence of phosphine reductants. *Bioconjug. Chem.* **27**: 2260–2265.
46. Richard, JP, Melikov, K, Vives, E, Ramos, C, Verbeure, B, Gait, MJ, *et al.* (2003). Cell-penetrating peptides A reevaluation of the mechanism of cellular uptake. *J. Biol. Chem.* **278**: 585–590.
47. Lundberg, M, Wikström, S and Johansson, M (2003). Cell surface adherence and endocytosis of protein transduction domains. *Mol. Ther.* **8**: 143–150.
48. Nakase, I, Tadokoro, A, Kawabata, N, Takeuchi, T, Katoh, H, Hiramoto, K, *et al.* (2007). Interaction of arginine-rich peptides with membrane-associated proteoglycans is crucial for induction of actin organization and macropinocytosis. *Biochemistry* **46**: 492–501.
49. De Bruin, K, Ruthardt, N, Von Gersdorff, K, Bausinger, R, Wagner, E, Ogris, M, *et al.* (2007). Cellular dynamics of EGF receptor–targeted synthetic viruses. *Mol. Ther.* **15**: 1297–1305.
50. Thiele, L, Rothen-Rutishauser, B, Jilek, S, Wunderli-Allenspach, H, Merkle, HP and Walter, E

(2001). Evaluation of particle uptake in human blood monocyte-derived cells in vitro. Does phagocytosis activity of dendritic cells measure up with macrophages? *J. Control. Release* **76**: 59–71.

51. Swanson, JA and Watts, C (1995). Macropinocytosis. *Trends Cell Biol.* **5**: 424–428.
52. Iwasaki, T, Tokuda, Y, Kotake, A, Okada, H, Takeda, S, Kawano, T, *et al.* (2015). Cellular uptake and in vivo distribution of polyhistidine peptides. *J. Control. Release* **210**: 115–124.
53. Watkins, CL, Schmaljohann, D, Futaki, S and Jones, AT (2009). Low concentration thresholds of plasma membranes for rapid energy-independent translocation of a cell-penetrating peptide. *Biochem. J.* **420**: 179–191.
54. Hoang, B, Ernsting, MJ, Roy, A, Murakami, M, Undzys, E and Li, S-D (2015). Docetaxel-carboxymethylcellulose nanoparticles target cells via a SPARC and albumin dependent mechanism. *Biomaterials* **59**: 66–76.
55. Castro-Sanchez, L, Soto-Guzman, A, Navarro-Tito, N, Martinez-Orozco, R and Salazar, EP (2010). Native type IV collagen induces cell migration through a CD9 and DDR1-dependent pathway in MDA-MB-231 breast cancer cells. *Eur. J. Cell Biol.* **89**: 843–852.
56. Ozdener, GB, Bais, M V and Trackman, PC (2016). Determination of cell uptake pathways for tumor inhibitor lysyl oxidase propeptide. *Mol. Oncol.* **10**: 1–23.
57. Kosuge, M, Takeuchi, T, Nakase, I, Jones, AT and Futaki, S (2008). Cellular Internalization and Distribution of Arginine-Rich Peptides as a Function of Extracellular Peptide Concentration , Serum , and Plasma Membrane Associated Proteoglycans: 656–664.
58. Tünnemann, G, Ter-Avetisyan, G, Martin, RM, Stöckl, M, Herrmann, A and Cardoso, MC (2008). Live-cell analysis of cell penetration ability and toxicity of oligo-arginines. *J. Pept. Sci.* **14**: 469–476.
59. Furuhata, M, Kawakami, H, Toma, K, Hattori, Y and Maitani, Y (2006). Design, synthesis and gene delivery efficiency of novel oligo-arginine-linked PEG-lipids: Effect of oligo-arginine length. *Int. J. Pharm.* **316**: 109–116.
60. Takayama, K, Tadokoro, A, Pujals, S, Nakase, I, Giralt, E and Futaki, S (2009). Novel system to achieve one-pot modification of cargo molecules with oligoarginine vectors for intracellular delivery. *Bioconjug. Chem.* **20**: 249–257.
61. Wimley, WC and White, SH (1996). Experimentally determined hydrophobicity scale for proteins at membrane interfaces. *Nat. Struct. Mol. Biol.* **3**: 842.
62. Matsubara, T, Iida, M, Tsumuraya, T, Fujii, I and Sato, T (2008). Selection of a Carbohydrate-Binding Domain with a Helix− Loop− Helix Structure. *Biochemistry* **47**: 6745–6751.
63. Kosuge, M, Takeuchi, T, Nakase, I, Jones, AT and Futaki, S (2008). Cellular internalization and distribution of arginine-rich peptides as a function of extracellular peptide concentration, serum, and plasma membrane associated proteoglycans. *Bioconjug. Chem.* **19**: 656–664.
64. Shankar, J and Nabi, IR (2015). Actin cytoskeleton regulation of epithelial mesenchymal transition in metastatic cancer cells. *PLoS One* **10**: e0119954.
65. Hijazi, MM, Thompson, EW, Tang, C, Coopman, P, Torri, JA, Yang, D, *et al.* (2000). Heregulin regulates the actin cytoskeleton and promotes invasive properties in breast cancer cell lines. *Int. J. Oncol.* **17**: 629–670.
66. Peela, N, Sam, FS, Christenson, W, Truong, D, Watson, AW, Mouneimne, G, *et al.* (2016). A three dimensional micropatterned tumor model for breast cancer cell migration studies. *Biomaterials* **81**: 72–83.

67. Lagana, A, Vadnais, J, Le, PU, Nguyen, TN, Laprade, R, Nabi, IR, *et al.* (2000). Regulation of the formation of tumor cell pseudopodia by the Na (+)/H (+) exchanger NHE1. *J. Cell Sci.* **113**: 3649–3662.
68. Walenga, RW, Opas, EE and Feinstein, MB (1981). Differential effects of calmodulin antagonists on phospholipases A2 and C in thrombin-stimulated platelets. *J. Biol. Chem.* **256**: 12523–12528.
69. Wells, A, Ware, MF, Allen, FD and Lauffenburger, DA (1999). Shaping up for shipping out: PLCγ signaling of morphology changes in EGF-stimulated fibroblast migration. *Cell Motil. Cytoskeleton* **44**: 227–233.
70. Kamiya, H, Akita, H and Harashima, H (2003). Pharmacokinetic and pharmacodynamic considerations in gene therapy. *Drug Discov. Today* **8**: 990–996.
71. El-Sayed, A, Khalil, IA, Kogure, K, Futaki, S and Harashima, H (2008). Octaarginine-and octalysine-modified nanoparticles have different modes of endosomal escape. *J. Biol. Chem.* **283**: 23450–23461.
72. Adams, JM and Cory, S (1998). The Bcl-2 protein family: arbiters of cell survival. *Science (80-.).* **281**: 1322–1326.
73. Karpel-Massler, G, Ishida, CT, Bianchetti, E, Shu, C, Perez-Lorenzo, R, Horst, B, *et al.* (2017). Inhibition of mitochondrial matrix chaperones and antiapoptotic Bcl-2 family proteins empower antitumor therapeutic responses. *Cancer Res.* **77**: 3513–3526.
74. Chipuk, JE, Moldoveanu, T, Llambi, F, Parsons, MJ and Green, DR (2010). The BCL-2 family reunion. *Mol. Cell* **37**: 299–310.
75. Youle, RJ and Strasser, A (2008). The BCL-2 protein family : opposing activities that mediate cell death **9**: 47–60.
76. Eskes, R, Desagher, S, Antonsson, B and Martinou, J-C (2000). Bid induces the oligomerization and insertion of Bax into the outer mitochondrial membrane. *Mol. Cell. Biol.* **20**: 929–935.
77. Wei, MC, Lindsten, T, Mootha, VK, Weiler, S, Gross, A, Ashiya, M, *et al.* (2000). tBID, a membrane-targeted death ligand, oligomerizes BAK to release cytochrome c. *Genes Dev.* **14**: 2060–2071.
78. Youle, RJ (2007). Cellular demolition and the rules of engagement. *Science (80-.).* **315**: 776–777.
79. Szakács, G, Paterson, JK, Ludwig, JA, Booth-Genthe, C and Gottesman, MM (2006). Targeting multidrug resistance in cancer. *Nat. Rev. Drug Discov.* **5**: 219.
80. Kuwana, T, Bouchier-Hayes, L, Chipuk, JE, Bonzon, C, Sullivan, BA, Green, DR, *et al.* (2005). BH3 domains of BH3-only proteins differentially regulate Bax-mediated mitochondrial membrane permeabilization both directly and indirectly. *Mol. Cell* **17**: 525–535.
81. Chen, L, Willis, SN, Wei, A, Smith, BJ, Fletcher, JI, Hinds, MG, *et al.* (2005). Differential targeting of prosurvival Bcl-2 proteins by their BH3-only ligands allows complementary apoptotic function. *Mol. Cell* **17**: 393–403.
82. Goldsmith, KC, Liu, X, Dam, V, Morgan, BT, Shabbout, M, Cnaan, A, *et al.* (2006). BH3 peptidomimetics potently activate apoptosis and demonstrate single agent efficacy in neuroblastoma. *Oncogene* **25**: 4525–4533.
83. Berridge, M V, Herst, PM and Tan, AS (2005). Tetrazolium dyes as tools in cell biology: new insights into their cellular reduction. *Biotechnol. Annu. Rev.* **11**: 127–152.

84. Isobe, I, Michikawa, M and Yanagisawa, K (1999). Enhancement of MTT, a tetrazolium salt, exocytosis by amyloid β-protein and chloroquine in cultured rat astrocytes. *Neurosci. Lett.* **266**: 129–132.
85. Śliwka, L, Wiktorska, K, Suchocki, P, Milczarek, M, Mielczarek, S, Lubelska, K, *et al.* (2016). The comparison of MTT and CVS assays for the assessment of anticancer agent interactions. *PLoS One* **11**: e0155772.
86. Lobner, D (2000). Comparison of the LDH and MTT assays for quantifying cell death: validity for neuronal apoptosis? *J. Neurosci. Methods* **96**: 147–152.
87. Hwang, T-L, Hsu, C-Y, Aljuffali, IA, Chen, C-H, Chang, Y-T and Fang, J-Y (2015). Cationic liposomes evoke proinflammatory mediator release and neutrophil extracellular traps (NETs) toward human neutrophils. *Colloids Surfaces B Biointerfaces* **128**: 119–126.
88. Roursgaard, M, Knudsen, KB, Northeved, H, Persson, M, Christensen, T, Kumar, PEK, *et al.* (2016). In vitro toxicity of cationic micelles and liposomes in cultured human hepatocyte (HepG2) and lung epithelial (A549) cell lines. *Toxicol. Vitr.* **36**: 164–171.
89. Dinca, A, Chien, W-M and Chin, MT (2016). Intracellular delivery of proteins with cell-penetrating peptides for therapeutic uses in human disease. *Int. J. Mol. Sci.* **17**: 263.
90. Elmore, S (2007). Apoptosis: a review of programmed cell death. *Toxicol. Pathol.* **35**: 495–516.
91. Riccardi, C and Nicoletti, I (2006). Analysis of apoptosis by propidium iodide staining and flow cytometrydoi:10.1038/nprot.2006.238.
92. Crowley, LC, Marfell, BJ, Scott, AP and Waterhouse, NJ (2016). Quantitation of apoptosis and necrosis by annexin V binding, propidium iodide uptake, and flow cytometry. *Cold Spring Harb. Protoc.* **2016**: pdb-prot087288.
93. Sanchez-Alcazar, JA, Ault, JG, Khodjakov, A and Schneider, E (2000). Increased mitochondrial cytochrome c levels and mitochondrial hyperpolarization precede camptothecin-induced apoptosis in Jurkat cells. *Cell Death Differ.* **7**: 1090.
94. Tan, C, Cai, L-Q, Wu, W, Qiao, Y, Imperato-McGinley, J, Chen, G-Q, *et al.* (2009). NSC606985, a novel camptothecin analog, induces apoptosis and growth arrest in prostate tumor cells. *Cancer Chemother. Pharmacol.* **63**: 303–312.
95. Zeng, C-W, Zhang, X-J, Lin, K-Y, Ye, H, Feng, S-Y, Zhang, H, *et al.* (2012). Camptothecin induces apoptosis in cancer cells via microRNA-125b-mediated mitochondrial pathways. *Mol. Pharmacol.* **81**: 578–586.
96. De Andrade, CR, Stolf, BS, Debbas, V, Rosa, DS, Kalil, J, Coelho, V, *et al.* (2011). Quiescin sulfhydryl oxidase (QSOX) is expressed in the human atheroma core: possible role in apoptosis. *Vitr. Cell. Dev. Biol.* **47**: 716–727.
97. Tünnemann, G, Martin, RM, Haupt, S, Patsch, C, Edenhofer, F and Cardoso, MC (2006). Cargo-dependent mode of uptake and bioavailability of TAT-containing proteins and peptides in living cells. *FASEB J.* **20**: 1775–1784.